



Contents lists available at ScienceDirect

Tectonophysics

journal homepage: www.elsevier.com/locate/tecto

Styles of lithospheric extension controlled by underplated mafic bodies

Tadashi Yamasaki^{a,b,*}, Laurent Gernigon^c

^a Dublin Institute for Advanced Studies, 5 Merrion Square, Dublin 2, Ireland

^b Department of Tectonics, Faculty of Earth and Life Sciences, VU University, Amsterdam, De Boelelaan 1085, 1081 HV Amsterdam, Netherlands

^c Norges Geologiske Undersøkelse (NGU/Geological Survey of Norway), leiv, Eirikssons vei 39, N-7491 Trondheim, Norway

ARTICLE INFO

Article history:

Received 30 August 2007

Received in revised form 2 April 2008

Accepted 22 April 2008

Available online xxxx

Keywords:

Localization of deformation

Underplated mafic bodies

Lithospheric rheology

Continental rift

Passive margin

Continental break-up

ABSTRACT

The role of underplated mafic bodies (UPMB) in the localization of deformation is examined using a two-dimensional thermo-mechanical finite element model. Rheological heterogeneity brought about by the UPMB is linked with the following two main physical effects: the UPMB material is assumed to have (1) an anomalous high temperature and (2) a mafic crustal rock composition that is intrinsically weaker than the mantle. The thermal effect will disappear rather quickly, but the rock composition can have an effect at any stage of extension. We show that the UPMB has a strong influence on the style of lithospheric extension, which depends on the thermal condition of the uppermost mantle at the time when the UPMB is emplaced. Since the strength contrast between the weakened and non-weakened regions is the most important factor, the UPMB works more efficiently on the localization of deformation for a colder uppermost mantle. Dependence of the localization of deformation on the temperature and thickness of the UPMB (i.e. more significant localization for the UPMB with higher temperature and greater thickness) also depends on the thermal condition of the uppermost mantle.

However, the width of the UPMB has a strong influence on the localization for any thermal condition of the uppermost mantle; a greater amount of thinning is distributed into a narrower weakened region. Such a model behaviour implies that various styles of lithospheric extension, including inward or outward migration of deformation and asymmetric extension, can be simply obtained by considering the emplacement of the UPMB, which also plays an important role in controlling the onset of continental break-up.

© 2008 Elsevier B.V. All rights reserved.

1. Introduction

Many continental rifts and passive margins display a high level of volcanic activity (see Fig. 1), before, during or shortly after extension (e.g., Ruppel, 1995; Neumann et al., 1995; White and McKenzie, 1989; Symonds et al., 1998; Gladchenko et al., 1997; Eldholm et al., 2000; Berndt et al., 2001; Menzies et al., 2002; Geoffroy, 2005; Mackenzie et al., 2005). The presence of high seismic velocity lower crust ($V_p \sim 7.1 \sim 7.8$ km/s) often observed along volcanic margins (Planke et al., 1991; Eldholm et al., 2000; Bauer et al., 2000; Mjelde et al., 2007) and magmatic rifts (e.g., Ro and Faleide, 1992; Mohr, 1992) is referred to as mantle-derived mafic intrusions, or so-called magmatic underplating (Cox, 1980; Mutter et al., 1984) or magmatic inflation (Thompson and McCarthy, 1990). Such underplated mafic bodies (UPMB) have been discussed in relation to (i) the high grade metamorphism of lower crustal material (e.g., Rey, 1993), (ii) thickening of the crust (Gans, 1987; Mohr, 1992), (iii) permanently higher post-rift topography (Lachen-

brunch and Sass, 1978, 1990; Lister et al., 1991) and (iv) significant positive gravity anomalies (Hutchinson et al., 1990).

However, in most kinematic and dynamic models of rift formation and evolution, the effects of magmatism have been neglected (e.g. McKenzie 1978; Royden and Keen 1980; Wernicke, 1985; Braun and Beaumont 1987; Buck 1991; Davis and Kusznir, 2004). The generation of melt associated with rifting has been investigated for a given kinematic model of extension, but without considering effect of melts on the dynamics (e.g., McKenzie and Bickle, 1988; White and McKenzie, 1989; Latin and White, 1990; Harry et al., 1993; Harry and Leeman, 1995). As many prior studies have emphasized that most of the rifted margins are affected by magmatism (e.g., Gernigon et al., 2004; Geoffroy, 2005; Ebbing et al., 2006; Gernigon et al., 2006; Lizarralde et al., 2007), one of the most important issues to address is how magmatic activity influences the rifting dynamics.

The aim of the present study is principally to evaluate, using a two-dimensional thermo-mechanical finite element model, the possible influence of UPMBs on localizing extensional deformation. The understanding of the development of continental rifts and passive margins requires knowledge of a process to explain how the deformation is localized. Continental rifts formed by large-scale extensional tectonics are characterized by locally thinned crust and high surface heat flows (e.g., Artemjev and Artyushkov, 1971; McKenzie, 1978). Continental

* Corresponding author. Department of Tectonics, Faculty of Earth and Life Sciences, VU University, Amsterdam, De Boelelaan 1085, 1081 HV Amsterdam, Netherlands. Tel: +31 20 5983921; fax: +31 20 5989943.

E-mail address: tadashi.yamasaki@falw.vu.nl (T. Yamasaki).

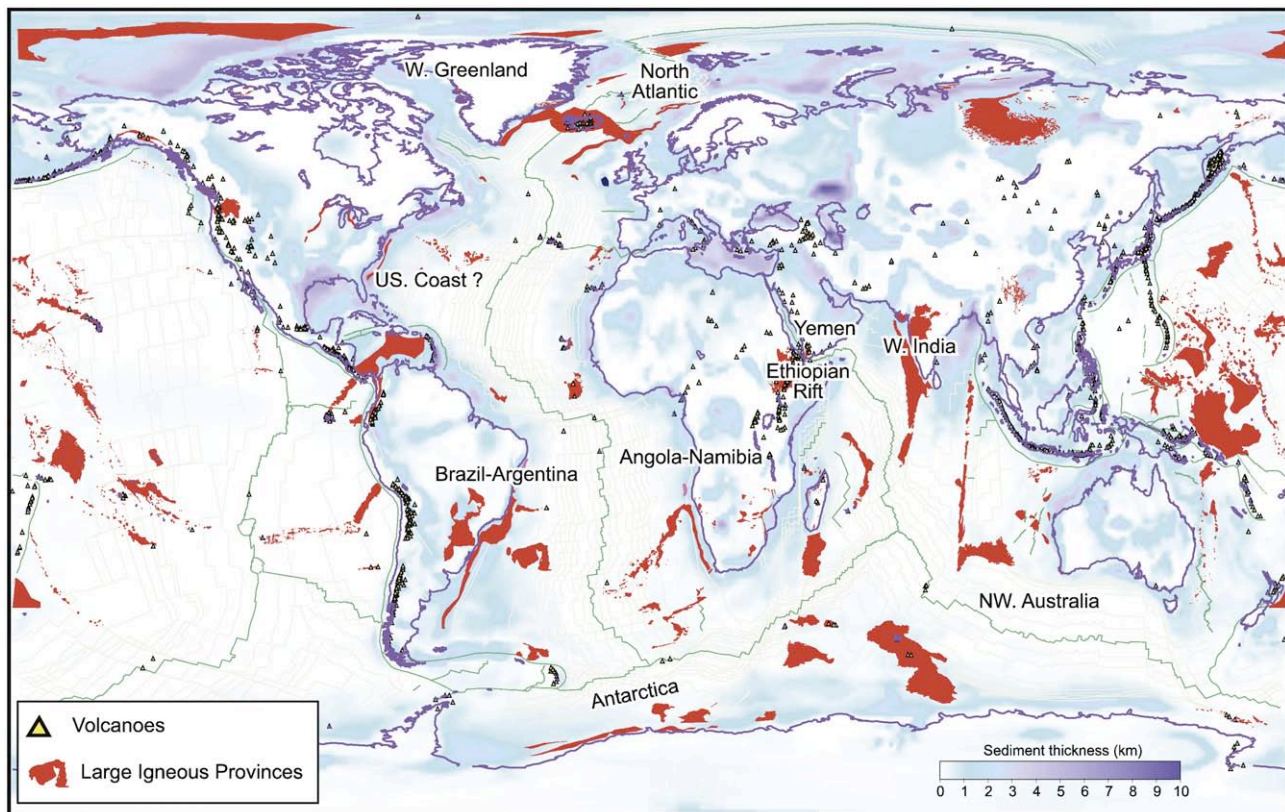


Fig. 1. Distribution of sedimentary basins, large igneous provinces, the main volcanic rifts and volcanic rifted margins in the world. This map illustrates the importance of the magmatism associated with sedimentary basins, continental margin and rift systems. Data after Coffin and Eldholm (1994) and Laske and Masters (1997). Isochrons are after Müller et al. (1997).

break-up is an end product of continental extension, and the break-up point usually focuses and concentrates within a local area (e.g., Ebinger and Casey, 2001). Thus, the problem which we also have to consider is what controls the localization of deformation. In this study, we focus on the UPMB as a possible origin of rheological heterogeneity, and attempt to investigate specifically a correlation between magmatism and rifting dynamics from the point of view of the localization of deformation. As well as the rheological heterogeneities brought about by a locally thickened crust (e.g., Braun and Beaumont, 1987; Bassi, 1991; Bassi et al., 1993; Govers and Wortel, 1993; Bassi, 1995; Govers and Wortel, 1995), temperature variation in the lithosphere (e.g., Govers and Wortel, 1999; Pascal et al., 2002) or pre-existing faults (e.g., Braun and Beaumont, 1989; Dunbar and Sawyer, 1988; 1989a,b; Melosh and Williams, 1989; Williams and Richardson, 1991), the presence of UPMBs in the continental lithosphere is likely to modify the thermal structure and mechanical properties (e.g., Frey et al., 1998; Buck, 2006), which could then control the evolution of the rift system. Analogue modelling studies by Callot et al. (2001, 2002) have previously demonstrated that localization can be brought about by low viscosity bodies in the lower crust and/or the uppermost mantle, interpreted as plume-related partial melts. Corti et al. (2003a) and Corti et al. (2007) also carried out analogue modelling experiments to investigate effects of melts on the progression of continental rifting into localized break-up. However, even though one of the most important physical mechanisms in such soft point models depends on temperature, it is difficult to include a temperature-dependent rheology in analogue modelling. Therefore, it is important to investigate the role of the UPMB in relation to its thermal aspects using numerical modelling (e.g., Gac and Geoffroy, submitted for publication).

This study particularly considers in detail the likely rheological heterogeneity brought about by the UPMB. We first discuss the role of the UPMB as the initial rheological heterogeneity, while respecting the initial crustal and thermal structure of the lithosphere. Since magmatic activity possibly precedes rifting (e.g., Burke and Dewey, 1973; Sengör and

Burke, 1978; Griffiths and Campbell, 1991; Menzies et al., 2002; Courtillot and Renne, 2003), the UPMB could work as the initial rheological heterogeneity. In fact, Buck (2006) emphasized the importance of magmatic intrusion as a possible means of reducing the entire lithospheric strength to initiate the rifting with a reasonable tectonic force.

The basic characteristics of the UPMB, i.e. its width, thickness and temperature are specifically examined in this study, as well as the relative importance of the UPMB to a locally thickened crust for the localization of deformation. Whether the lateral variation in the thickness of the UPMB has the potential to bring about the asymmetric structures found in rift and passive margins is also examined in this study. We lastly demonstrate the possible localization of deformation that can be brought about by the UPMB during the extensional process.

2. Model description

The two-dimensional finite element model is schematically shown in Fig. 2. We examine the response of the lithosphere to an applied constant boundary velocity at the edge of the model. The UPMB is introduced as a material with an anomalous high temperature and mafic lower crustal composition. The mechanical problem is coupled with the thermal problem through temperature-dependent viscosity. The plane strain condition, which seems appropriate for the geological structure of a rift, is assumed in this study. The lithosphere has three compositional layers: wet quartzite upper crust, anorthite lower crust, and wet dunite mantle.

The origin of the force driving the extension is not considered. Even if the lithosphere has a uniform rheological structure localization of deformation can be obtained by a non-uniform driving force. The rising plume may control a location where deformation could be concentrated (e.g., Sengör and Burke, 1978; Burov and Guillou-Frottier, 2005; Burov et al., 2007). Additionally, in the laboratory analogue model of Tirel et al. (2006), localization of deformation is obtained by a

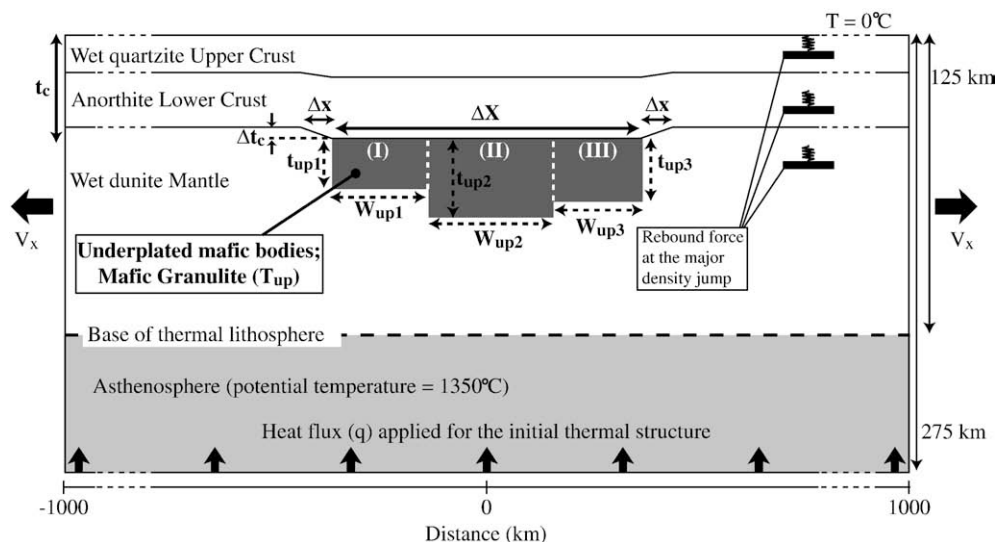


Fig. 2. Schematic figure of the numerical model adopted in this study. The continental lithosphere has three compositional layers: wet quartzite upper crust, anorthite lower crust and wet dunite mantle. The initial thickness of the crust is t_c , and the thickness of the lower crust is $t_c/2$. A constant horizontal boundary velocity ($V_x = 1$ cm/year) is applied at the right and left side ends of the model. The Winkler restoring force is applied at the following major density interfaces so as to calculate the vertical surface movements: at the surface, the boundary between upper and lower crust and at the Moho. The thermal boundary condition of the model is as follows. The horizontal heat flow is zero at the right and left side boundaries of the model. The temperature of the surface is fixed to be 0°C . In order to obtain the steady state solution of Eq. (5) the reduced heat flow is applied at the bottom of the model, satisfying the condition that the temperature at the base of a given thermal lithosphere (at a depth of 125 km) is equal to the potential temperature of the asthenosphere (1350°C). At depths below the thermal lithosphere the temperature is set to be the potential temperature of the asthenosphere. In the transient thermal problem, the temperature below the depth of 125 km is imposed to be 1350°C as a constant temperature boundary condition. Three domains of the UPMB (I–III) with abnormally high temperature and mafic lower crustal composition are characterized by W_{up1} and t_{up1} , W_{up2} and t_{up2} , and W_{up3} and t_{up3} , respectively. All domains of the UPMB are assumed to have uniform temperature T_{up} . For the model with a locally thickened crust, the crust is thickened by $\otimes t_c$ over a distance $\otimes X$ in the centre of the model. The transition from thickened to normal crust takes place over a distance of $\otimes x$, and the Moho depth linearly decreases from t_c to $t_c - \otimes t_c$ (km). The initial topographic height resulting from the isostatic response to the thickened crust is not taken into account in the setup of the model.

velocity discontinuity between the surrounding rigid plates and the plate in which deformation is taking place. In the present study, however, localization of deformation is particularly discussed in relation to the rheological heterogeneity brought about by the UPMB, so that we just apply a constant velocity ($V_x = 1$ cm/yr) at the left and right side boundaries of the model.

Since the formation process of UPMBs is still poorly understood, we simply assume that the UPMB is emplaced instantaneously, as is adopted in Frey et al. (1998), without considering how the melt is generated and how it migrates upwards. Additionally, even though both the timing of the emplacement and volume of the UPMB are important factors in controlling magma related heterogeneities (e.g., Chapman and Furlong, 1992), it is still difficult to exactly estimate the timing of the magmatism and the quantity of generated melt prior to and/or during extension. For example, as shown in Hirth and Kohlstedt (1996), the process of decompressional melting cannot be investigated without information of the initial water content in the mantle peridotite. Therefore we make simple assumptions about the timing and distribution of the UPMB.

The UPMB is described by three basic parameters, its width (W_{up}), thickness (t_{up}) and temperature (T_{up}). Each of three domains of the UPMB (labelled I, II and III in Fig. 2) are characterized by W_{up1} and t_{up1} , W_{up2} and t_{up2} , and W_{up3} and t_{up3} , respectively. All the domains are assumed to have a uniform temperature T_{up} .

In this study, the UPMB is regarded as the primal origin of rheological heterogeneity for localization of deformation. However, the rheological heterogeneity brought about by a locally thickened crust is also a plausible origin of the heterogeneity, as adopted in many prior studies (e.g., Braun and Beaumont, 1987; Bassi, 1991; Bassi et al., 1993; Govers and Wortel, 1993; Bassi, 1995; Govers and Wortel, 1995). Therefore, we perform several models with a locally thickened crust in the Section 3.4 in order to investigate the condition where the UPMB could play a dominant role in localizing the deformation. For the model with a locally thickened crust, the continental lithosphere has a crustal thickness t_c locally thickened by $\otimes t_c$ over a distance $\otimes X$ in the

centre of the model (see Fig. 2). The transition from thickened to normal crust takes place over a distance of $\otimes x$, over which the Moho depth linearly decreases from t_c to $t_c - \otimes t_c$. The initial topographic height resulting from the isostatic response to the thickened crust is not taken into account in the setup of the model. A finite element code, tekton ver. 2.1, developed by Melosh and Raefsky (1980, 1981) and Melosh and Williams (1989), is used to solve the mechanical equilibrium equation

$$\nabla \cdot \sigma + X = 0 \quad (1)$$

where σ is the stress tensor and X is the body force. Large strain and displacement effects are incorporated by using an updated Lagrangian method. The vertical movements of the major density interfaces, i.e. the surface, the boundary between the upper and lower crust, and the Moho, are calculated by using the Winkler restoring force (e.g., Williams and Richardson, 1991). The constitutive relationships that relate the stress to the strain are required to solve the mechanical equilibrium equation. The viscoelastic-perfect plastic rheology model with temperature-dependent viscosity has been incorporated into the code (Yamasaki et al., submitted for publication). Under low deviatoric stress conditions, rock deformation is elastic, in which the strain is linearly related to the stress by the generalized Hooke's law (e.g., Ranalli, 1995). However, under larger deviatoric stress conditions, different deformation mechanisms become more important, depending on the temperature and pressure conditions.

Under low temperature and pressure conditions, deformation of rocks takes place in a brittle manner. The brittle stress σ_b is given by Byerlee's law (Byerlee, 1967, 1978):

$$\sigma_b = \zeta (1 - v^*) z \quad (2)$$

where z is the depth in km, ζ is a constant (24 MPa/km) and v^* (0.4) is the density ratio of pore water to rock matrix (e.g., Brace and Kohlstedt, 1980; Ranalli, 1995). The elastic-perfect plastic rheology is adopted for the brittle deformation (e.g., Flecher and Hallet, 1983; 201

Braun and Beaumont, 1987; Bassi, 1995). The state of the stress is assumed to be controlled by the Von Mises yield criterion F ,

$$F = J_{2D}^{-\frac{1}{3}} \sigma_y^2 = 0 \quad (3)$$

where J_{2D} is the second invariant of deviatoric stress and σ_y is the yield stress that is equivalent to σ_b in Eq. (2).

On the other hand, under high temperature and pressure conditions, ductile deformation is the dominant mechanism. A non-linear Maxwell viscoelastic rheology is adopted for the ductile behaviour of rocks (e.g., Melosh and Raefsky, 1980; Braun and Beaumont, 1987; Bassi, 1995; Govers and Wortel, 1995). The viscous flow is controlled by power law creep (e.g., Kirby, 1983; Carter and Tsenn, 1987), where the effective viscosity η can be written in the form

$$\eta = \frac{1}{2A^*} J_{2D}^{\frac{1-n}{2}} \exp\left(\frac{Q}{R\theta}\right) \quad (4)$$

where A^* is a material constant, Q is the activation energy, n is the stress exponent, R is the universal gas constant and θ is the absolute temperature. Flow law parameters of each rock composition are shown in Table 1.

Since power law creep is a function of temperature, the distribution of temperature in the lithosphere must be calculated at all stages of deformation. The time-dependent heat conduction equation is given by

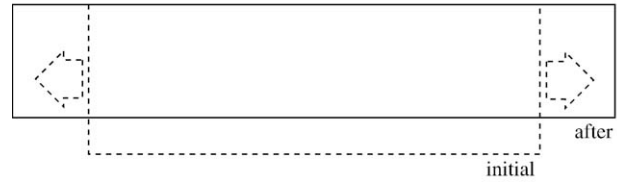
$$\rho C_p \frac{\partial T}{\partial t} = \nabla \cdot (K \nabla T) + H \quad (5)$$

where ρ is the density, C_p is the specific heat, T is the temperature, t is the time, K is the thermal conductivity and H is the radiogenic heat

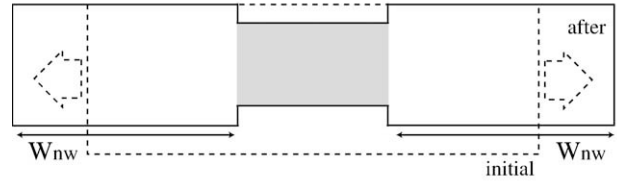
Table 1
Model parameter values used in this study

Symbol	Meaning	Value
E	Young's modulus	1.5×10^{11} Pa
ν	Poisson's ratio	0.25
ζ	Depth dependence of brittle failure	24.0 MPa/km
ν^*	Density ratio of pore water to rock	0.4
C_p	Specific heat	$1050 \text{ J kg}^{-1} \text{ K}^{-1}$
R	Universal gas constant	$8.314 \text{ J mol}^{-1} \text{ K}^{-1}$
T_a	Potential temperature of the asthenosphere	$1350 \text{ }^\circ\text{C}$
T_s	Temperature at the surface	$0 \text{ }^\circ\text{C}$
ρ_{uc}	Mass density of the upper crust	2800 kg m^{-3}
ρ_{lc}	Mass density of the lower crust	2900 kg m^{-3}
ρ_m	Mass density of the mantle	3300 kg m^{-3}
H_{uc}	Heat production in the upper crust	$1.37 \text{ } \mu\text{W m}^{-3}$
H_{lc}	Heat production in the lower crust	$0.45 \text{ } \mu\text{W m}^{-3}$
H_m	Heat production in the mantle	$0.02 \text{ } \mu\text{W m}^{-3}$
K_{uc}	Thermal conductivity of the upper crust	$2.56 \text{ W m}^{-1} \text{ K}^{-1}$
K_{lc}	Thermal conductivity of the lower crust	$2.60 \text{ W m}^{-1} \text{ K}^{-1}$
K_m	Thermal conductivity of the mantle	$3.20 \text{ W m}^{-1} \text{ K}^{-1}$
Flow law parameters of power law creep		
Wet quartzite: Koch et al. (1989)		
A_{uc}^*	Pre-exponent	$1.10000 \times 10^{-21} \text{ Pa} \cdot \text{ns}^{-1}$
n_{uc}	Power	2.61
Q_{uc}	Activation energy	145 kJ mol^{-1}
Anorthite: Shelton and Tullis (1981)		
A_{lc}^*	Pre-exponent	$5.60000 \times 10^{-23} \text{ Pa} \cdot \text{ns}^{-1}$
n_{lc}	Power	3.20
Q_{lc}	Activation energy	238 kJ mol^{-1}
Wet Aheim dunite: Chopra and Paterson (1984)		
A_m^*	Preexponent	$5.4954 \times 10^{-25} \text{ Pa} \cdot \text{ns}^{-1}$
n_m	Power	4.48
Q_m	Activation energy	498 kJ mol^{-1}
Mafic granulite: Ranalli (1995)		
A_{upmb}^*	Preexponent	$8.8334 \times 10^{-22} \text{ Pa} \cdot \text{ns}^{-1}$
n_{upmb}	Power	4.2
Q_{upmb}	Activation energy	445 kJ mol^{-1}

(a) Uniform lithosphere (no lateral rheological heterogeneity)



(b) Weak heterogeneity



(c) Strong heterogeneity

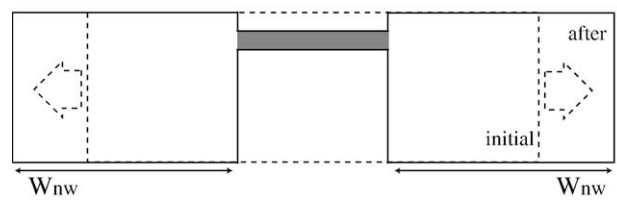


Fig. 3. Localization of extensional deformation; (a) extension of the uniform lithosphere with no lateral rheological heterogeneity, (b) extension of the lithosphere with weak rheological heterogeneity, and (c) extension of the lithosphere with strong rheological heterogeneity.

We ignore the effect of the latent heat associated with the solidification of melts. Parameter values used in this study are shown in Table 1. We have written an additional finite element code to solve the transient heat conduction equation (Eq. (5)). Overlapping thermal and mechanical finite element grids are used to solve the heat and mechanical equilibrium equations sequentially. Advection of heat is incorporated in a way that the finite element geometry is updated every time step with the displacements computed by the mechanical algorithm. The thermal boundary conditions are as follows. At the left and right side boundaries of the model the horizontal heat flow is zero. The temperature at the surface is held at $0 \text{ }^\circ\text{C}$. The potential temperature of the asthenosphere is assumed to be $1350 \text{ }^\circ\text{C}$. The initial thermal structure is calculated from the steady-state solution of Eq. (5). The reduced heat flow is applied to satisfy the condition that the temperature at the base of the thermal lithosphere (at a depth of 125 km) is equal to the potential temperature of the asthenosphere (i.e. the thickness of the thermal lithosphere a is defined by the $1350 \text{ }^\circ\text{C}$ isotherm). Below a depth of 125 km, the temperature is assumed to be identical to the asthenospheric potential temperature. In the transient thermal problem, the temperature at a depth greater than 125 km is imposed to be $1350 \text{ }^\circ\text{C}$ as a constant temperature boundary condition.

3. Results and discussion

Extensional deformation of the lithosphere results in its thinning following the conservation of mass. If a lithosphere that has no lateral rheological heterogeneities is extended by an applied boundary velocity, thinning of the lithosphere will occur uniformly (see Fig. 3(a)). However, if lateral rheological heterogeneity is present in the lithosphere, the thinning will be distributed, particularly into a weak region (e.g., Fernández and Ranalli, 1997). In this case, the strength contrast of the heterogeneity is an important factor in controlling how much of the thinning is distributed into the weak region. If the strength contrast is

258 weak, there will be a small amount of thinning in the weak region
 259 because extension is also significantly accommodated by thinning in the
 260 non-weakened region (Fig. 3(b)). On the other hand, for a stronger
 261 strength contrast, extensional deformation is mostly accommodated by
 262 thinning the weak region (see Fig. 3(c)). It should be noted that in the
 263 numerical model the strength contrast is, in practice, recognized by the
 264 difference in the strain rate. Higher strain rate is obtained in the
 265 weakened region, which results in the localization of deformation.

266 We have confirmed that the least amount of a thinning of the
 267 lithosphere cannot be avoided in the non-weakened region even for
 268 the model with significant strength contrast. Extension applied at the
 269 edge of the model is also accommodated by a thinning of the non-
 270 weakened region, and the total amount of extension accommodated
 271 in the non-weakened region increases as W_{nw} (width of non-
 272 weakened region) increases. That is, the amount of thinning
 273 distributed into the weakened region becomes smaller for the
 274 model with larger W_{nw} . Therefore, the absolute amount of thinning
 275 in a significantly deformed region can be evaluated only for a specific

size of model. The most important point to be investigated is the
 sensitivity to an assumed heterogeneity.

3.1. Dependence on the initial lithospheric structure

Rheological heterogeneity brought about by the UPMB is linked with
 the following two physical effects: (1) the higher temperature of the
 UPMB results in weakening through the temperature-dependence of the
 viscosity and (2) the mafic crustal composition of the UPMB is
 significantly weaker than the mantle, even without any thermal effects.

Fig. 4(a) and (b) shows the initial temperature distributions for the
 models with and without the UPMB, with $t_c=30$ and 40 km,
 respectively. The temperature at the Moho is higher for the model
 with $t_c=40$ km than for the model with $t_c=30$ km. Therefore, the
 difference in temperature between the UPMB and normal mantle is
 larger for the model with $t_c=30$ km than for the model with $t_c=40$ km.

This implies that the UPMB could be more effective in localizing
 the deformation for the model with $t_c=30$ km. When t_c is 30 km, the

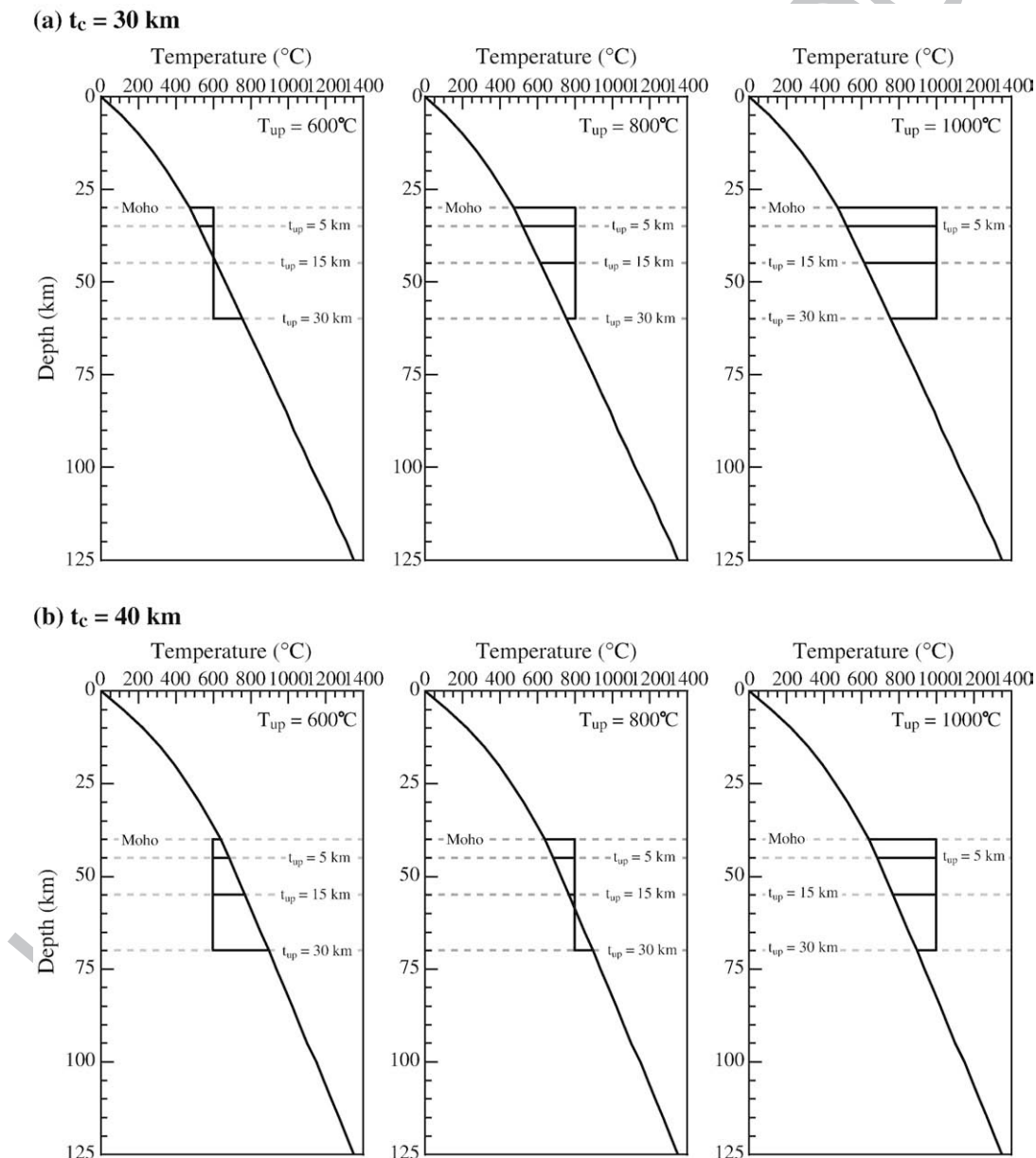


Fig. 4. Temperature distributions for the models with and without an UPMB that has an abnormal temperature T_{up} ($T_{up}=600, 800$ and 1000 °C) and a thickness of t_{up} ($t_{up}=5, 15$ and 30 km); (a) $t_c=30$ km and (b) $t_c=40$ km.

292 temperature of the UPMB for the model with $T_{up}=800$ and 1000 °C is
 293 greater than that of the normal mantle from the Moho to the base of
 294 the UPMB. For the model with $T_{up}=600$ °C, the temperature of the

UPMB is higher than that of normal mantle to a depth of about 45 km,
 295 but lower at a greater depth. When t_c is 40 km, with $T_{up}=600$ °C the
 296 temperature of the UPMB is never higher than that of the uppermost
 297

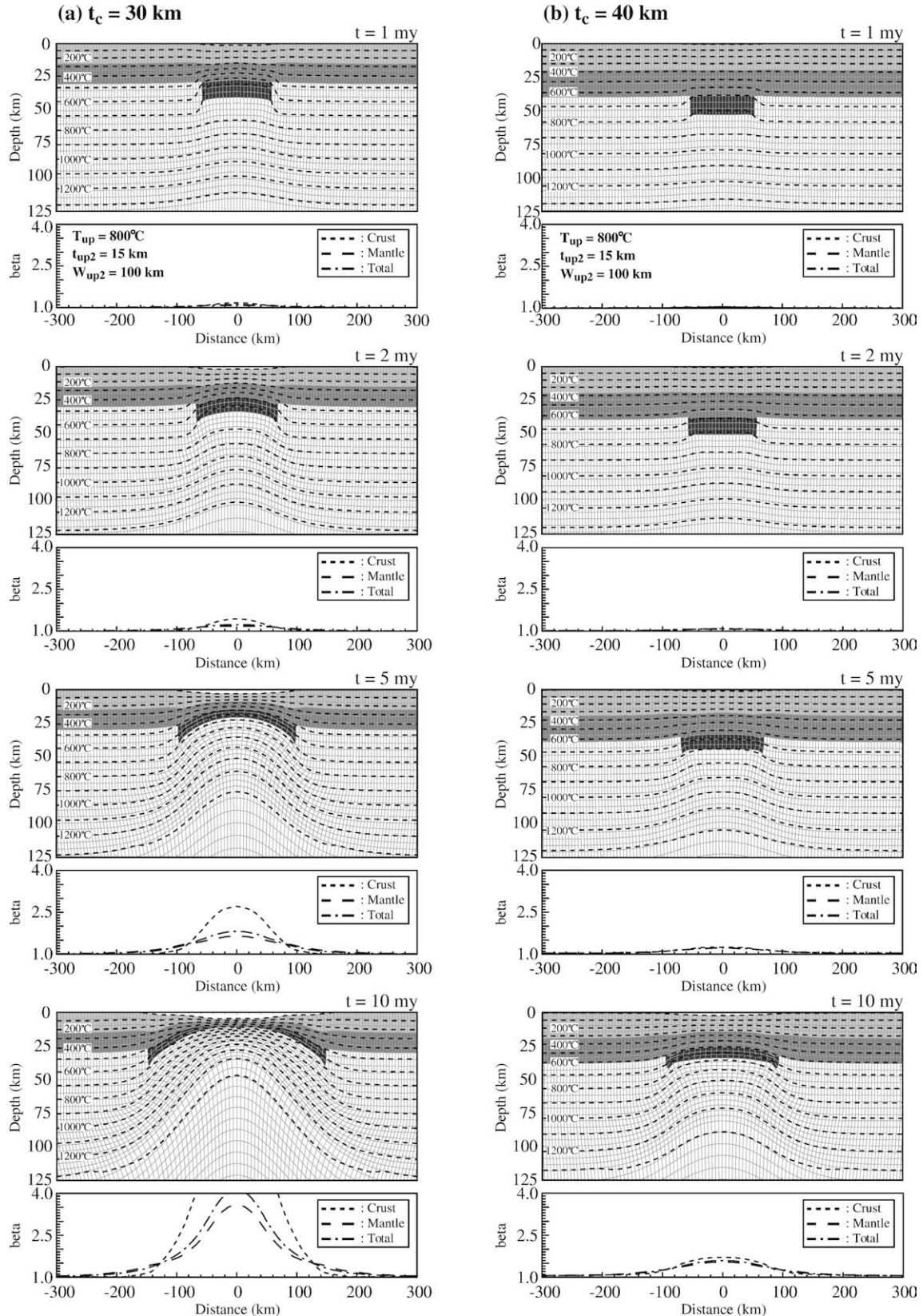


Fig. 5. Time-dependent deformed grids with superimposed temperature contours for the UPMB models with $\otimes t_c = 0$ km, $W_{up1} = W_{up3} = 0$ km, $W_{up2} = 100$ km and $T_{up2} = 800$ °C; (a) $t_c = 30$ km and (b) $t_c = 40$ km. Contours of temperature are shown at 100 °C intervals from 0 to 1300 °C. Stretching factors of the crust (dotted curve), mantle (dashed curve) and total (dotted and dashed curve) are depicted for each time. The stretching factor is defined by the ratio of the thickness before extension to the thickness after extension.

mantle for the whole range of t_{up} . Even for the model with $T_{up}=800\text{ }^{\circ}\text{C}$, the temperature is higher only to a depth of about 55 km. However, for the model with $T_{up}=1000\text{ }^{\circ}\text{C}$, the UPMB results in a higher temperature anomaly over the whole depth range where the UPMB is situated.

Fig. 5(a) and (b) shows the extensional deformation of the lithosphere with increasing time for the models with $t_c=30$ and 40 km, respectively, in which only the centre domain (II) is used to describe the characteristic of the UPMB (i.e. $W_{up1}=W_{up3}=0$). A locally thickened crust prior to extension is not taken into account ($\otimes t_c=0$ km). It is assumed that T_{up} is 800 $^{\circ}\text{C}$, W_{up2} is 100 km and $t_{up2}=15$ km. It can be clearly seen that a greater amount of thinning is distributed into a weakened region for the model with $t_c=30$ km than for the model with $t_c=40$ km. The total stretching factor at time $t=10$ my reaches up to about 4.0 for the model with $t_c=30$ km, but to only about 1.6 for the model with $t_c=40$ km. A greater strength reduction through the increase in temperature is obtained by the UPMB for the model with $t_c=30$ km because of the smaller initial geothermal gradient in the normal mantle (see Fig. 4).

It should be also noted that the temperature anomaly caused by the UPMB disappears within a few million years. The period that the UPMB can keep a temperature higher than the normal mantle may practically depend on the size of the UPMB and the time-scale of its formation process (e.g., Chapman and Furlong, 1992): the period could be shorter for a smaller UPMB and/or for a slower formation of the UPMB. On the other hand, another effect relating to the difference in composition between the UPMB and mantle could work on localizing deformation at any stage of extension, because this effect has no relation to temperature.

Although only the results of the model with $a=125$ km are shown, the UPMB model is applicable for any thicknesses of the thermal lithosphere. Since the localization of the deformation brought about by the UPMB is dependent on the degree of strength reduction, it is

clear that the UPMB works more effectively for the colder lithosphere than for the hotter lithosphere.

3.2. The basic model parameters describing the characteristics of the UPMB

Fig. 6 shows how the stretching factor varies as a function of distance for models with $t_c=30$ km and 40 km, in which only the domain II is used to describe the characteristic of the UPMB. A locally thickened crust prior to extension is not taken into account ($\otimes t_c=0$ km). The times are 6 and 10 my for the models with $t_c=30$ and 40 km, respectively. Fig. 6(a) shows the dependence of extensional deformation on T_{up} , with $W_{up2}=100$ km and $t_{up2}=15$ km. Three models are shown for $T_{up}=600, 800$ and $1000\text{ }^{\circ}\text{C}$. The dependence on T_{up} is not seen in the model with $t_c=30$ km. Even when the temperature of the UPMB is 600 $^{\circ}\text{C}$, the temperature anomaly necessary to produce a strength contrast strong enough to distribute the thinning mostly into a weak zone is obtained below the Moho (see Fig. 4(a)). On the other hand, for the model with $t_c=40$ km, the localization of the deformation is dependent on T_{up} ; a higher UPMB temperature leads to a higher degree of thinning distributed into a weak region, because the strength contrast between weakened and non-weakened regions is larger for higher UPMB temperature. It is also important to note that extensional deformation can be localized even for the model with $t_c=40$ km and $T_{up}=600\text{ }^{\circ}\text{C}$, i.e. the temperature of the UPMB is lower than that of the normal mantle (Fig. 4(b)). This is because the mafic crustal material is intrinsically weaker than the mantle without any thermal effects.

Fig. 6(b) shows the dependence on t_{up2} , with $W_{up2}=100$ km and $T_{up}=800\text{ }^{\circ}\text{C}$, for models with $t_{up2}=5, 15$ and 30 km. When t_c is 40 km, a greater amount of thinning is distributed into a weak zone for the models with greater t_{up2} . A greater reduction in the total lithospheric

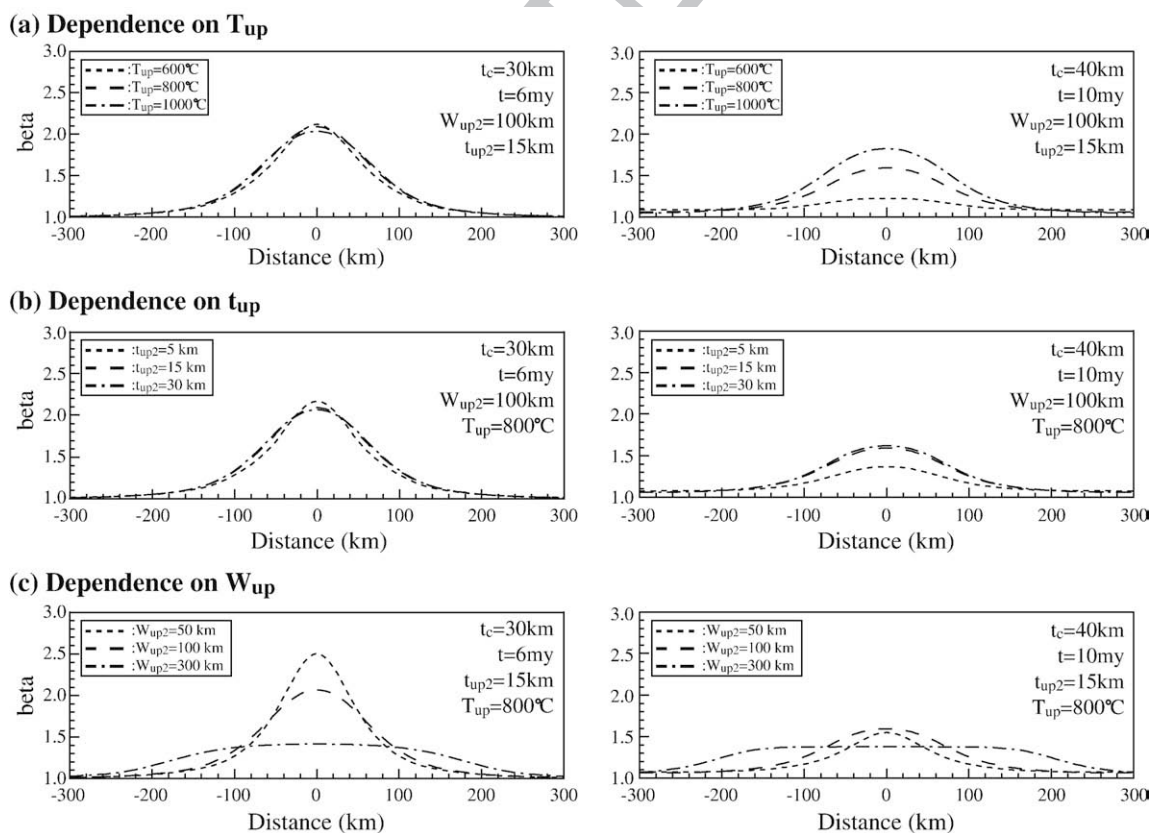


Fig. 6. Total stretching factors as a function of a distance for different (a) T_{up} , (b) t_{up2} and (c) W_{up2} , in which $\otimes t_c=0$ km and $W_{up1}=W_{up3}=0$ km. Times are 10 and 6 my for the models with $t_c=30$ and 40 km, respectively.

360 strength is obtained by the model with greater t_{up2} . This is consistent with
361 the results from analogue modelling by Corti et al. (2007).

362 However, the temperature of the UPMB becomes lower than the
363 mantle temperature at a depth greater than ~ 57 km (see Fig. 4(b)), so
364 that at a further depth it becomes difficult to obtain the significant
365 strength reduction by the temperature anomaly of the UPMB. In fact,
366 models with $t_{up2} \geq 15$ km do not further enhance the localization of the
367 deformation, in which the stretching factor predicted by the model with
368 $t_{up2} = 15$ km is almost the same as that with $t_{up2} = 30$ km. On the other
369 hand, when t_c is 30 km, the model behaviour is virtually independent of
370 t_{up2} . Even for the model with $t_{up2} = 5$ km the strength contrast is strong
371 enough to distribute the thinning mostly into a weak region.

372 Fig. 6(c) shows the dependence on W_{up2} , with $t_{up2} = 15$ km and
373 $T_{up} = 800$ °C. The results of the models with $W_{up2} = 50, 100$ and 300 km
374 are depicted in the figures. As Corti et al. (2007) demonstrated
375 previously using an analogue model, our numerical model also shows
376 a strong dependence on W_{up2} for both $t_c = 30$ and 40 km. A greater
377 amount of thinning is distributed into a weak region for the models
378 with smaller W_{up2} . For a given amount of extension at the boundary of
379 the model, the extensional deformation of the lithosphere is
380 accommodated by the distribution of thinning into a narrower region
381 for the model with smaller W_{up2} , which leads to a higher strain rate in
382 deformed region.

383 3.3. Localization of deformation by slow strain rate or UPMB in the lower 384 crust: outward migration of deformation

385 As described above, the distribution of thinning into a weak region
386 is controlled by the rheological heterogeneity introduced as a result of

the presence of the UPMB. Our model shows that distribution of
387 thinning into a weak zone is larger for the models with stronger
388 strength contrast and with a narrower UPMB. Consequently, the strain
389 rate in the significantly deformed zone is controlled by the
390 characteristics of the UPMB, i.e. even if the applied boundary velocity
391 is fixed, various strain rates can be obtained. 392

It is important to discuss the effect of strain rate on the extensional
393 deformation in relation to thermal diffusion. The strength of the
394 lithosphere changes as extension progresses, as a result of the
395 competition between the weakening caused by the increase in
396 geothermal gradient associated with the passive upwelling of the
397 asthenosphere and the strengthening by crustal thinning and thermal
398 diffusion. For a smaller strain rate, the strengthening by thermal
399 diffusion becomes the more dominant factor (e.g., England, 1983). 400

Fig. 7(a) shows the result of the model with an UPMB in which
401 $W_{up1} = W_{up3} = 0$, $W_{up2} = 300$ km, $t_{up2} = 30$ km and $T_{up} = 800$ °C. A locally
402 thickened crust prior to extension is not taken into account
403 ($\otimes t_c = 0$ km). It can be seen that lithospheric thinning moves outward
404 in the later rifting phase. Similar numerical model behaviour has been
405 reported by van Wijk and Cloetingh (2002) and Corti et al. (2003b), in
406 which outward migration of the thinning was obtained by a model
407 with a low extensional velocity or a very wide thickened crust. Such
408 model behaviour is attributed to the thermal diffusion in a deformed
409 region with a slow strain rate. For the model with $W_{up2} = 300$ km,
410 extensional deformation is accommodated by a distribution of
411 thinning into a wide weak region, so that the obtained strain rate is
412 low and the effect of thermal diffusion plays an important role in the
413 style of extension. On the other hand, the strain rate in the deformed
414 region for the models with $W_{up2} \leq 150$ km is so high (see Figs. 5 and 6) 415

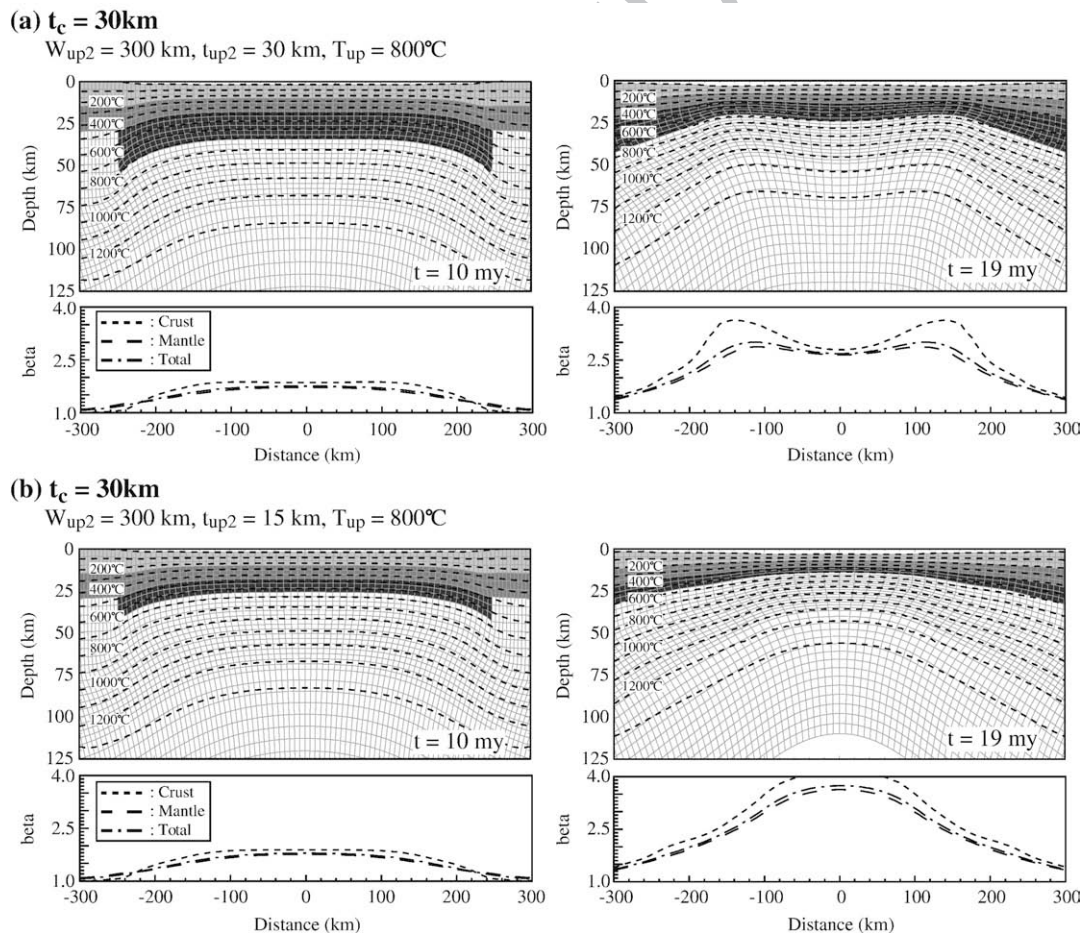


Fig. 7. Deformed grids with superimposed temperature contours for the model with $t_c = 30$ km, $\otimes t_c = 0$ km, $W_{up1} = W_{up3} = 0$ km, $W_{up2} = 300$ km and $T_{up} = 800$ °C at $t = 10$ and 19 my; (a) $t_{up2} = 30$ km and (b) $t_{up2} = 15$ km. Stretching factors of the crust (dotted curve), mantle (dashed curve) and total (dotted and dashed curve) are depicted for each model.

that it is difficult to obtain outward migration by thermal diffusion. Fig. 7(b) shows the result of setting $t_{up2} = 15$ km. Outward deformation migration is not obtained by this model. This result indicates that the replacement of the mafic lower crustal material (the UPMB) with mantle material is also an important factor in controlling the change in the total lithospheric strength. The replacement is smaller for the model with smaller t_{up2} . Therefore, even though the thermal diffusion progresses significantly, the centre of the rift does not become strong enough to obtain outward migration of deformation.

Prior numerical modelling studies have successfully explained an outward migration of deformation in terms of thermal diffusion in the deformed region (e.g., Negrodo et al., 1995; van Wijk and Cloetingh, 2002; Corti et al., 2003b). However, if the UPMB is taken into account, it is generally difficult to obtain migration of the deformation to outside the UPMB region, because the UPMB has intrinsically less strength than the mantle without considering the thermal effects. Even if outward migration of deformation can be obtained by the model with the UPMB, its migration is limited to the region where the UPMB is present (see Fig. 7(a)). Therefore, in order to shift deformation to outside the UPMB region, there may be no other way than by considering a shift of magmatic activity, such as following a change in plume activity (Müller et al., 2001; Yamada and Nakada, 2006).

Only the UPMB in the uppermost mantle just below the Moho has been examined in this study. However it is likely that melts could intrude into the lower crust (e.g., Bonini et al., 2001; Corti et al., 2003a). We give an important implication for the case of the UPMB in the lower crust. As described above, the UPMB has the two physical properties important for the localization of deformation: it has an abnormally high temperature and an intrinsically weaker composition than the mantle. Because mafic granulite has a greater strength than anorthite lower crust (e.g., Ranalli, 1995; Ranalli et al., 2007), the compositional effect does not work if the UPMB is situated in the lower crust. Once the temperature anomaly caused by the UPMB in the lower crust is significantly relaxed by thermal diffusion, deformation would be localized into outside the UPMB where the felsic lower crust is intrinsically weaker than the UPMB. In the prior analogue modelling studies on extensional deformation of the lithosphere in relation to the magmatic process (Callot et al., 2001; 2002; Corti et al., 2003a; Corti et al., 2003b; Corti et al., 2007), the origin of the localization of deformation is brought about by a low viscosity body not only in the mantle but also in the lower crust. However it might be questionable to keep such a low viscosity body in the lower crust over the entire duration of rifting.

3.4. Relative importance of the UPMB to a locally thickened crust

Fig. 8 shows a relative importance of the UPMB to a locally thickened crust in which $\otimes X$ and $\otimes x$ are 100 and 25 km, respectively. Only the domain II with $t_{up2} = 15$ km and $T_{up} = 800$ °C is used to describe the characteristic of the UPMB. The time is 6 my for all models. Fig. 8(a) shows the results with $t_c = 30$ km and $\otimes t_c = 5$ km. For the model without the UPMB, the total stretching factor is predicted to be about 2.2, at most. On the other hand, for a UPMB with $W_{up2} = 50$ km, the stretching factor at the centre of the rift reaches 2.6, which is significantly larger than that for the model without the UPMB. However, an UPMB model with $W_{up2} = 100$ km predicts an almost identical stretching factor to that predicted by the model without the UPMB (~ 2.2). In addition, the stretching factor at the centre decreases to 1.8 for the model with $W_{up2} = 300$ km.

Fig. 8(b) shows the results for the model with $t_c = 30$ km and $\otimes t_c = 2.5$ km. The predicted stretching factor at the centre for the model without the UPMB is smaller than that even for the UPMB model with $W_{up2} = 300$ km. This is because a difference in t_c of 2.5 km does not result in a strength contrast strong enough to distribute thinning mostly into a region weakened by a locally thickened crust.

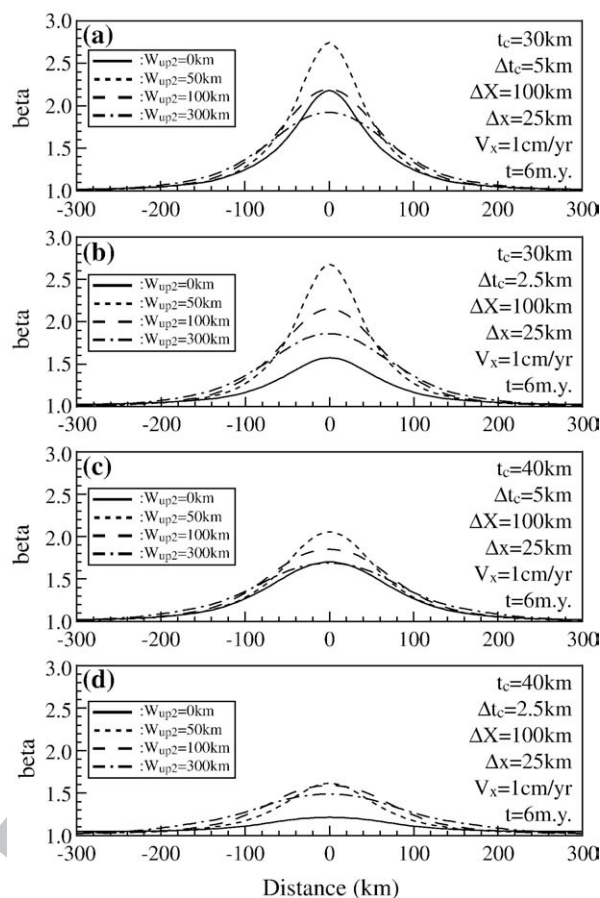


Fig. 8. Total stretching factors as a function of a distance for different widths (W_{up2}) of an UPMB, at $t = 6$ my, with $\otimes X = 100$ km and $\otimes x = 25$ km; (a) $t_c = 30$ km and $\otimes t_c = 5$ km, (b) $t_c = 30$ km and $\otimes t_c = 2.5$ km, (c) $t_c = 40$ km and $\otimes t_c = 5$ km, and (d) $t_c = 40$ km and $\otimes t_c = 2.5$ km. It is assumed that $W_{up1} = W_{up3} = 0$ km, $t_{up2} = 15$ km and $T_{up} = 800$ °C.

The obtainable strength contrast for the model with $t_c = 40$ km is weaker than for the model with $t_c = 30$ km, as shown in the previous subsection. The same is true for the rheological heterogeneity by a locally thickened crust. Therefore, for a given amount of extension, the predicted stretching factor (the amount of thinning distributed into a weak region) for the model with $t_c = 40$ km is significantly smaller than that predicted for the model with $t_c = 30$ km (see Fig. 8(c) and (d)). For the model with $t_c = 40$ km, even when $\otimes t_c$ is assumed to be 5 km (see Fig. 8(c)), the stretching factor for the model without the UPMB is predicted to be only the same as that for the UPMB model with $W_{up2} = 300$ km. When $\otimes t_c$ is assumed to be 2.5 km (see Fig. 8(d)), the predicted stretching factor without the UPMB is significantly smaller than that obtained with the UPMB, which is practically independent of W_{up2} (at least for W_{up2} between 50 and 300 km).

Thus, if the lateral scale of the UPMB is smaller than that of a locally thickened crust, the UPMB plays a dominant role in localization of deformation. However, if the crustal thickness variation is small, the UPMB still plays a dominant role in localization of deformation which is independent on W_{up2} .

3.5. Inhomogeneous thickness of the UPMB: implication for asymmetric structure of continental rifts and passive margins

Fig. 9 shows the results of the models where the UPMB has a variable thickness. Only two domains of the UPMB are considered (i.e., $W_{up2} = 0$ km). T_{up} is assumed to be 800 °C for the both domains. A locally thickened crust prior to extension is not taken into account ($\otimes t_c = 0$ km). For the models with $W_{up1} = W_{up3} = 50$ km, $t_{up1} = 5$ km and $t_{up3} = 15$ km

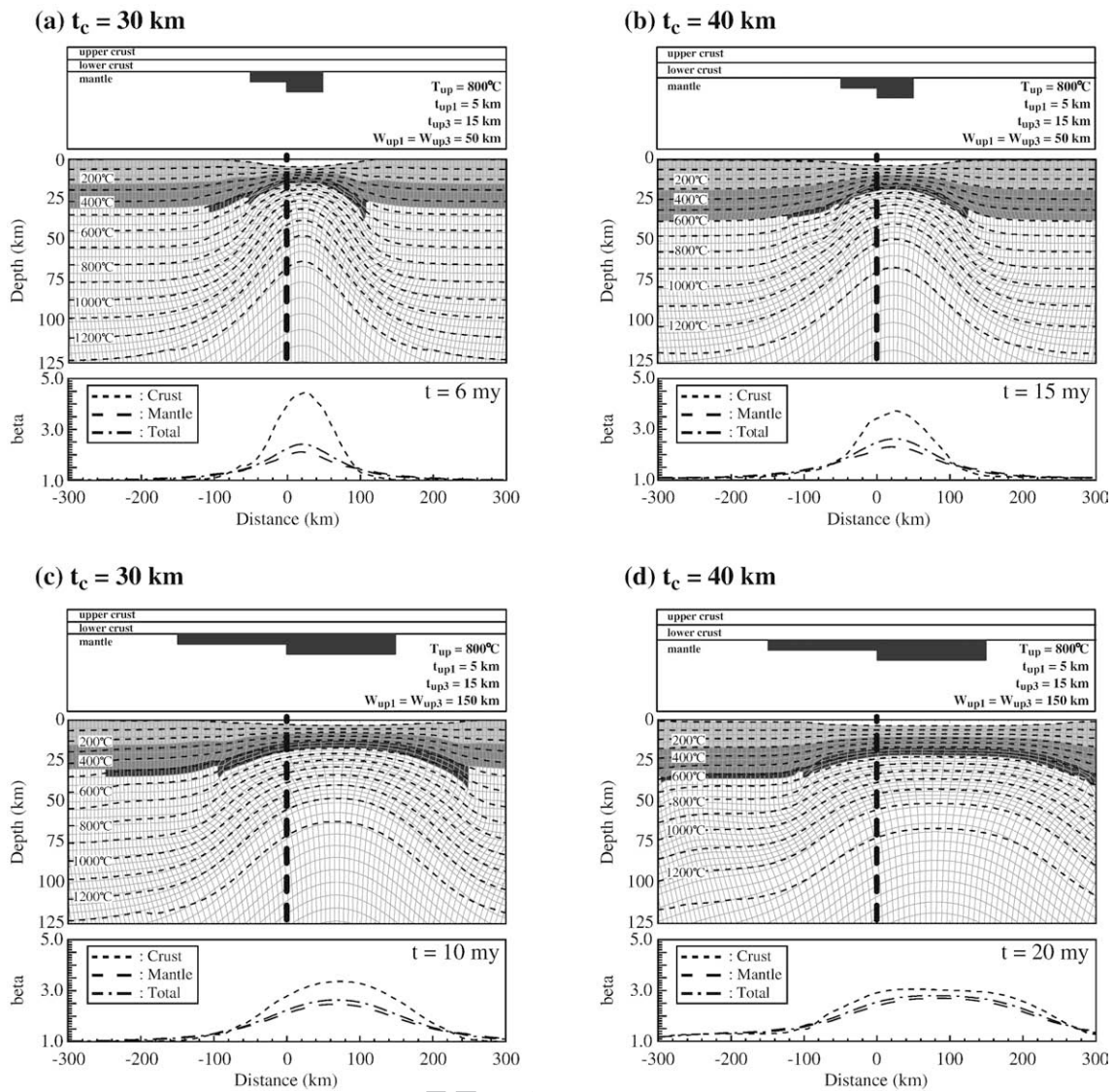


Fig. 9. Deformed grids with superimposed temperature contours for the model with $T_{up}=800\text{ }^{\circ}\text{C}$, $\otimes t_c=0\text{ km}$, $W_{up2}=0\text{ km}$, $t_{up1}=5\text{ km}$ and $t_{up3}=15\text{ km}$; (a) $t_c=30\text{ km}$ and $W_{up1}=W_{up3}=50\text{ km}$; (b) $t_c=40\text{ km}$ and $W_{up1}=W_{up3}=50\text{ km}$; (c) $t_c=30\text{ km}$ and $W_{up1}=W_{up3}=150\text{ km}$, and (d) $t_c=40\text{ km}$ and $W_{up1}=W_{up3}=150\text{ km}$. The vertical dotted line indicates the centre of the model. Stretching factors of the crust (dotted curve), mantle (dashed curve) and total (dotted and dashed curve) are shown for each model.

(see Fig. 9(a) and (b)), a greater amount of lithospheric thinning can be seen to be distributed into domain III (where there is a greater thickness of UPMB). The axis of the significantly deformed region is shifted from the centre of the model, producing an asymmetric structure about the centre of the model. However, the structure seems mostly symmetric about the axis of the significantly deformed region (although slight asymmetry is perceptible for the model with $t_c=40\text{ km}$).

For the models with $W_{up1}=W_{up3}=150\text{ km}$, the axis of the deformed region is shifted even more from the centre of the model (see Fig. 9(c) and (d)). For the model with $t_c=30\text{ km}$, the predicted structure still seems to be mostly symmetric about the axis of the significantly deformed region. The strength contrast between domains I and III is large enough to distribute a thinning into the domain III. On the other hand, for the model with $t_c=40\text{ km}$, a slight asymmetry about the axis of the significantly deformed region can be seen. Here the strength contrast between the two domains of the UPMB is not strong enough, so that a significant amount of thinning is distributed even into the domain I. The same physical explanation can be applied to the models with $W_{up1}=W_{up3}=50\text{ km}$. However, the lateral scale of the UPMB is too small for the asymmetric structure to be clearly perceptible (see Fig. 9(a) and (b)).

Fig. 10 shows results where three domains of the UPMB are taken into account with different thicknesses; $t_{up1}=5\text{ km}$, $t_{up2}=30\text{ km}$ and $t_{up3}=15\text{ km}$. T_{up} is assumed to be $800\text{ }^{\circ}\text{C}$ for all the domains. A locally thickened crust prior to extension is not taken into account ($\otimes t_c=0\text{ km}$). Fig. 10(a) and (b) shows the results of the models with $W_{up1}=W_{up2}=W_{up3}=50\text{ km}$. The maximum amount of thinning is now distributed into domain II, and the stretching factor becomes maximum in the centre of the model. The predicted structure is asymmetric about the centre of the model and also the axis of most deformed region.

The results of the models with $W_{up1}=120\text{ km}$, $W_{up2}=60\text{ km}$ and $W_{up3}=120\text{ km}$ are shown in Fig. 10(c) and (d). The stretching factor is again maximum at the centre of the model and is clearly asymmetric even about the centre of the model. Although the greatest amount of the thinning is distributed into domain II where the UPMB has the greatest thickness ($=30\text{ km}$), a significant thinning also spreads into domain III where t_{up2} is 15 km . The strength contrast between domain II and III is not large enough to localize deformation only into domain II, so that there is significant deformation even in domain III (especially for the model with $t_c=40\text{ km}$). For the model with $t_c=30\text{ km}$, significant thinning is not distributed into domain I, where

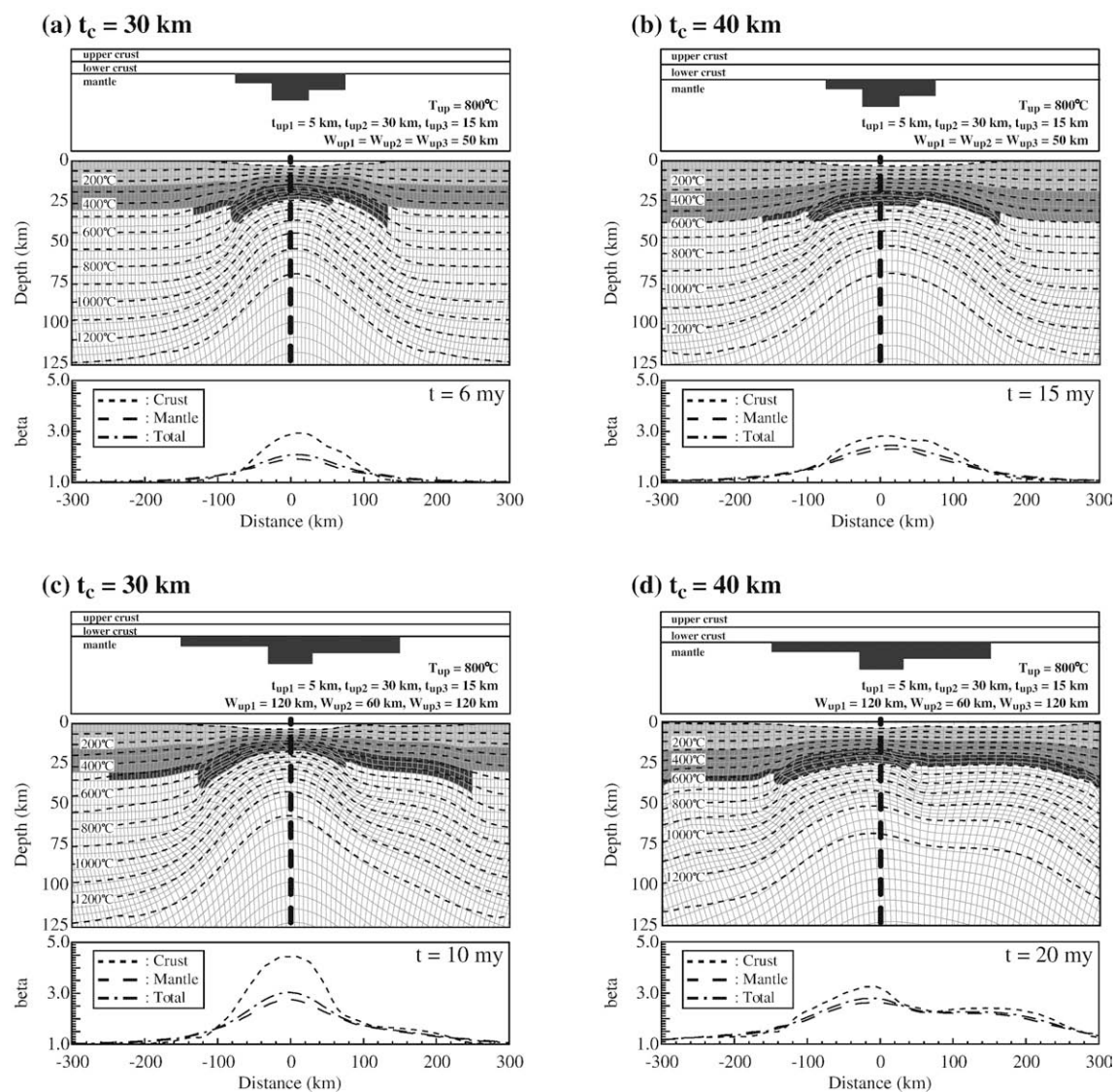


Fig. 10. Deformed grids with superimposed temperature contours for the model with $T_{up}=800^\circ\text{C}$, $\otimes t_c=0$ km, $t_{up1}=5$ km, $t_{up2}=30$ km and $t_{up3}=15$ km; (a) $t_c=30$ km and $W_{up1}=W_{up2}=W_{up3}=50$ km, (b) $t_c=40$ km and $W_{up1}=W_{up2}=W_{up3}=50$ km, (c) $t_c=30$ km, $W_{up2}=60$ km and $W_{up1}=W_{up3}=120$ km, and (d) $t_c=40$ km and $W_{up2}=60$ km and $W_{up1}=W_{up3}=120$ km. The vertical dotted line indicates the centre of the model. Stretching factors of the crust (dotted curve), mantle (dashed curve) and total (dotted and dashed curve) are shown for each model.

the UPMB has only a thickness of 5 km. The strength contrast between domain I and II is large enough to localize deformation into domain II. On the other hand, for the model with $t_c=40$ km, the strength contrast between the three domains of the UPMB is not high enough for significant thinning to be distributed, even into domain I.

In previous dynamic models, large-scale lithospheric deformation has been usually discussed in relation to the rheological change during the extensional process without considering the importance of the initial heterogeneities. However, Dunbar and Sawyer (1988, 1989a,b) proposed the important insight that the structure of the initial heterogeneity offers the key to understanding the development of continental extension. Corti et al. (2003b) and Corti and Manetti (2006) attempted to confirm this concept by using analogue and numerical models, in which the asymmetric geometry of passive margins, wide non-volcanic margins and narrow volcanic margins, are explained by an initial asymmetric structure of a locally thickened crust. In fact, clearly the asymmetric structure cannot be obtained by the symmetric initial setup of the model.

Similarly, as shown in this study, the asymmetric structure brought about by the inhomogeneous thickness of the UPMB might explain

wide non-volcanic and narrow volcanic margins, in which a greater amount of deformation focuses into the region where the UPMB has greater thickness.

However, this kind of asymmetry is basically obtained by the shift of the significantly deformed region from the centre of the UPMB, so that it is essentially required that the UPMB have its greatest thickness at a point that is significantly distant from the centre of the UPMB (see Fig. 9). In fact, if the greatest thickness of the UPMB is located at the centre of the UPMB, it becomes difficult to explain the characteristics of the wide and narrow passive margins (see Fig. 10).

Additionally, even if the UPMB has a variation in thickness, the structure of the rift seems to be mostly symmetric about the axis of the significantly deformed region for a small lateral scale of UPMB.

Therefore, the UPMB may have to range over a region wide enough to obtain a perceptible asymmetry.

It is also important to note that the asymmetric structure brought about by the inhomogeneous thickness of the UPMB can be clearly obtained when the strength contrast between each domain of the UPMB is weak enough not to distribute deformation into a particular domain.

588 Although the asymmetric structure of continental rifts and passive
 589 margins has been usually explained in terms of the simple shear
 590 model (Wernicke, 1985) or the combined pure and simple shear
 591 models (e.g., Kuszir and Egan, 1989; Lister and Davis, 1989; Lister
 592 et al., 1991), it is not necessary for the asymmetry to be accompanied
 593 by a large-scale shear zone in the lithosphere (e.g., Corti et al., 2003b;
 594 Corti and Manetti, 2006). Our numerical models also explain the
 595 asymmetric structure of extended lithosphere without the develop-
 596 ment of a shear zone cutting the lithosphere. The presence of a shear
 597 zone might be a consequence of asymmetry, rather than its origin.
 598 However, it may still be impossible that the initial asymmetric
 599 heterogeneity is sufficient to obtain the shear zone. Other sorts of
 600 rheological weakening during the extensional process may be
 601 required to develop a large-scale shear zone in the lithosphere (e.g.,
 602 Frederiksen and Braun, 2001; Huisman and Beaumont, 2002;
 603 Yamasaki, 2004; Yamasaki et al., 2006).

604 3.6. The UPMB during extension: from inward deformation migration to
 605 continental break-up

606 Fig. 11 shows localization of deformation brought about by the UPMB
 607 during the extensional process. A locally thickened crust is adopted so as
 608 to obtain an initial localization of deformation, where t_c is 40 km, $\otimes X$
 609 is 300 km, $\otimes x$ is 25 km and $\otimes t_c$ is 5 km. Only the domain II is used to
 610 describe the characteristic of the UPMB. It is assumed that the UPMB
 611 with $t_{up2} = 15$ km, $W_{up2} = 50$ km and $T_{up} = 800$ °C is emplaced at time
 612 $t = 5$ my. Extensional deformation prior to the onset of the UPMB is
 613 obviously controlled by the initial heterogeneity brought about by the
 614 locally thickened crust, and deformation takes place over a wide broad

region. However, once the UPMB is emplaced, the thinning is apparently
 615 distributed into a narrower region, following rheological weakening by
 616 the UPMB. The supply of magma decreases the lithospheric strength and
 617 localizes the deformation into the magmatic zone. 618

In the Ethiopian rift, where the development of continental rifting
 619 into sea-floor spreading is being demonstrated, inward deformation
 620 migration is observed. Showing that border faults are inactivated prior
 621 to continental break-up and most of the strain across the rift is
 622 accommodated in the magmatic segments, Ebinger and Casey (2001)
 623 has suggested that there is migration of extensional deformation into
 624 narrower magmatic segments in the rift. Then, Keranen et al. (2004)
 625 and Maguire et al. (2006) supported the view that extensional
 626 deformation in the Ethiopian rift is strongly controlled by magmatic
 627 activity, based on a crustal seismic velocity model combined with
 628 geological studies where the distribution of faults and dike deforma-
 629 tion zones were concentrated above high seismic velocity bodies,
 630 interpreted as intra-crustal and/or underplated intrusions. Keir et al.
 631 (2006) also pointed out a good correlation between the distributions
 632 of seismicities and magmatic activities, emphasizing an interaction
 633 between tectonic processes and magmatic activity. Similar character-
 634 istics of such an interaction between magmatism and tectonics can
 635 also be seen in Afar (e.g., Hayward and Ebinger, 1996; Manighetti et al.,
 636 1998; Doubré et al., 2007a,b), in the North Atlantic margin (e.g.,
 637 Gernigon et al., 2004; Geoffroy et al., 2001; Gernigon et al., 2006), in
 638 the northwest coast of Scotland (Speight et al., 1982) and in the
 639 Ligurian Tethys (Corti et al., 2007; Ranalli et al., 2007). 640

Our numerical results are consistent with these observations; 641
 642 inward migration of deformation can be explained by rheological
 643 heterogeneity brought about by the UPMB during the extensional 643

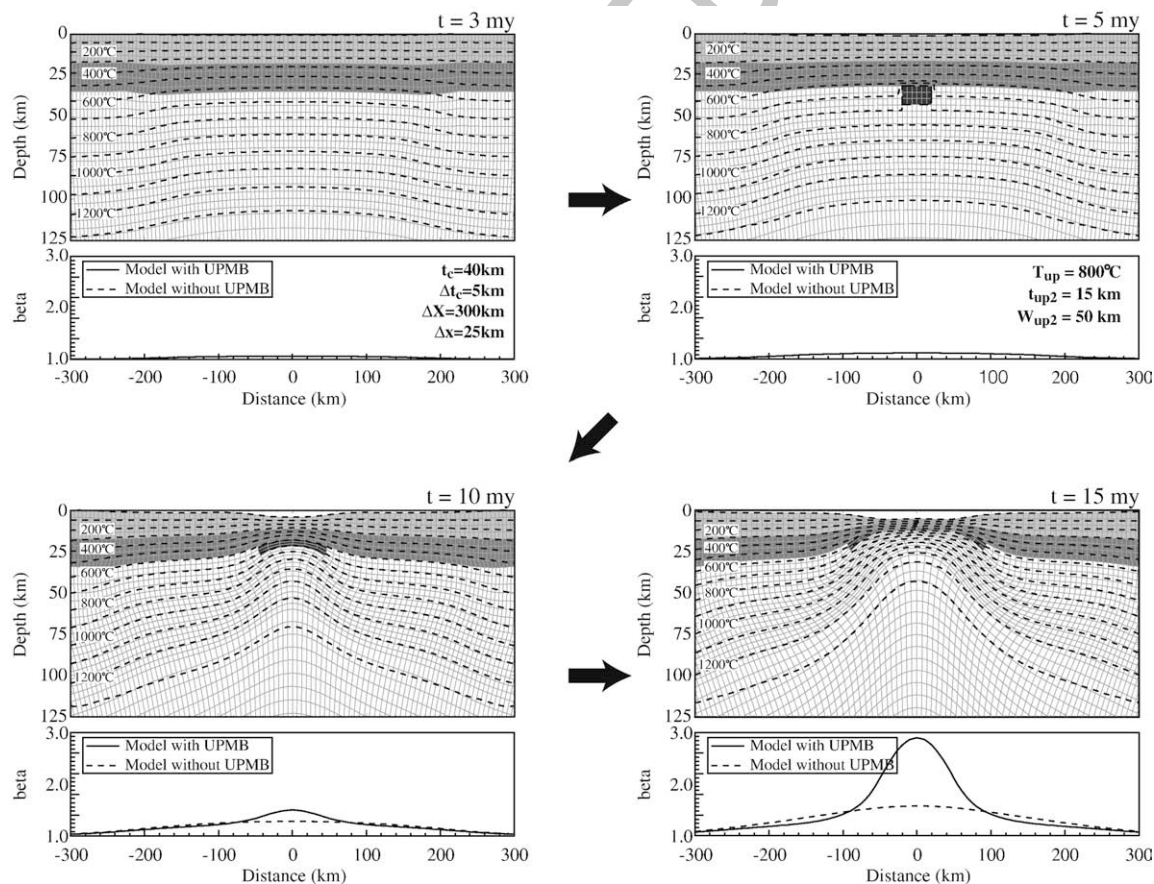


Fig. 11. Time-dependent extensional deformation of the lithosphere for the UPMB models with $W_{up1} = W_{up3} = 0$ km, $W_{up2} = 50$ km, $t_{up2} = 15$ km and $T_{up} = 800$ °C. For the initial crustal configuration, it is assumed that $\otimes X$ is 300 km, $\otimes x$ is 25 km and $\otimes t_c$ is 5 km. Emplacement of the UPMB is at $t = 5$ my. Stretching factors of the total lithosphere for the models with and without the UPMB are depicted for each time.

644 processes. We have discussed localization of deformation brought
 645 about by the UPMB in the particular case where an UPMB is present
 646 prior to the onset of extension. However, the general model behaviour
 647 obtained in the previous sections is applicable even to localization of
 648 deformation during the extensional process. It has been shown in this
 649 study that the UPMB works more efficiently to localize a deformation
 650 for originally colder uppermost mantle. It is also well known that any
 651 material within the lithosphere suffers cooling as the lithosphere
 652 thins. Therefore, the magmatic activity in later phases of the
 653 extensional process (i.e. after a deformed region has cooled down
 654 significantly by thermal diffusion) is more appropriate to localize
 655 deformation. In this regard, the UPMB could work on significant
 656 localization of deformation even for an initially hot lithosphere if the
 657 UPMB is emplaced during the extensional process.

658 It is also important to note that a small amount of magmatic
 659 emplacement is more favourable to the initiation of the localization of
 660 deformation, rather than a huge amount. In this study, and also in [Corti
 661 et al. \(2007\)](#), it is shown that a narrower UPMB can localize
 662 deformation more effectively. Additionally, as discussed above, even
 663 a thin UPMB could work efficiently on localization of deformation if an
 664 extended lithosphere is significantly cooled by thermal diffusion. A
 665 large amount of the UPMB may blur out the localization of deformation,
 666 and the deformation may range over a wide broad region (see
 667 [Figs. 6\(c\) and 7](#)). The break-up triggered by a magmatic process, even
 668 that observed in the magma poor margin of the Newfoundland–Iberia
 669 rift system ([Tucholke et al., 2007](#)), may be good evidence to support the
 670 view that a small amount of the UPMB is enough to bring about
 671 significant localization of deformation. Once the additional rheological
 672 heterogeneity brought about by the UPMB occurs, the thinning of the
 673 lithosphere may be increased and local magmatic activity enhanced,
 674 which in turn successively induces subsequent localizations of
 675 deformation and magmatic activity into a more local region.

676 Such a localization process could explain a sudden transition from
 677 continental rifting to break-up and subsequent enhancement of major
 678 magmatic activity at the break-up point. In the Outer Vøring Basin,
 679 where inward migration of the deformation during the onset of
 680 magmatism has also been documented by [Gernigon et al. \(2004\)](#),
 681 [Geoffroy et al. \(2001\)](#) and [Gernigon et al. \(2006\)](#), seismic observations
 682 show that faulting migrated towards the proto-oceanic rift during the
 683 onset of major magmatism in the Paleocene, indicating that the
 684 inward migration of the deformation started before the major volcanic
 685 phase during the ultimate continental break-up during the Late
 686 Palaeocene–Early Eocene. The emplacement of a small amount of
 687 UPMB might bring about the onset of the deformation migration, and
 688 a consequent increase in lithospheric thinning at the break-up point
 689 could cause major volcanic activity there. It may be more reasonable
 690 to regard the major volcanic phase at the break-up point to be a result
 691 of the localization of the deformation, because a huge amount of
 692 magmatic emplacement prior to the onset of the deformation
 693 migration may prevent the formation of a localized break-up point.

694 Many studies have emphasized the importance of dike intrusions
 695 on surface extensional tectonics (e.g., [Poliakov and Buck, 1998](#); [Ebinger
 696 and Casey, 2001](#); [Geoffroy et al., 2001](#); [Klausen and Larsen, 2002](#);
 697 [Keranen et al., 2004](#); [Sigmundsson, 2006](#); [Wright et al., 2006](#)).
 698 However, the process of dike intrusion may have the potential only
 699 to affect the deformation of the brittle upper crust (e.g., [Keranen et al.,
 700 2004](#)). Additionally, as pointed out above, an UPMB in the crust can
 701 possibly bring about an outward migration of deformation, which from
 702 the point of view of its compositional characteristics, has more
 703 strength than the continental crust. Therefore, it may be difficult to
 704 regard the diking process in the upper crust as the main factor in
 705 controlling the break-up process. The intrusion of dikes may be, rather,
 706 a complementary and secondary product of a significantly localized
 707 deformation that is brought about by an UPMB in the uppermost
 708 mantle. Extensional tectonics controlled by the dike intrusion may
 709 indicate the latest stage of the break-up, not its initiation.

4. Conclusions

710

711 In this study, we have investigated the influence of the UPMB on
 712 the style of lithospheric extension so as to discuss a correlation
 713 between magmatism and rifting dynamics. The numerical modelling
 714 study has demonstrated that UPMBs play an important role in
 715 controlling the localization of deformation, depending on the initial
 716 crustal and thermal structure of the lithosphere, the basic character-
 717 istics of the UPMB, the geometry of the UPMB, and the timing of the
 718 emplacement of the UPMB. This study also provides important
 719 insights into the dynamics of rifting and development of continental
 720 rifting into sea-floor spreading. It should be noted that the general
 721 model behaviour has been discussed mostly in the particular case
 722 where an UPMB is present prior to the onset of extension. However,
 723 such a model behaviour must be applicable even to the localization of
 724 deformation during extension. That is, the initial lithospheric condi-
 725 tion assumed in this study can be regarded as the condition at the time
 726 when the UPMB is emplaced. The model with an initially located
 727 UPMB evaluates only the minimum effect of the UPMB on localization
 728 of deformation. This is because each material point in the lithosphere
 729 being extended suffers cooling, and consequently the UPMB emplaced
 730 during extension leads to a greater decrease in strength. The limitation
 731 of our model is related to the assumption in which the UPMB is a
 732 solidified mafic lower crustal material, not a melt. Rheological prop-
 733 erty of a partially molten rock should be applied in a more realistic
 734 self-consistent model, which remains as a matter to be investigated in
 735 a future.

The main conclusions of the study are as follows:

736

- (i) The role of UPMBs in localization of deformation is linked with the
 737 following two main physical effects: they have an anomalously
 738 high temperature and a mafic crustal rock composition that has
 739 less strength than the mantle. The former effect will disappear
 740 rather shortly after the emplacement of the UPMB, but the latter
 741 one could play an important role at any stage of extension. 742
- (ii) The most important factor in controlling localization of
 743 deformation is the strength contrast between the weakened
 744 and non-weakened regions. The strength contrast brought
 745 about by the UPMB is strongly dependent on the thermal
 746 condition of the uppermost mantle at the time when the UPMB
 747 is emplaced; colder uppermost mantle results in a larger
 748 strength contrast. Thus, the UPMB will work more efficiently on
 749 the localization of deformation for colder uppermost mantle. 750
 Dependence on the characteristics of the UPMB is also
 751 dependent on the thermal condition of the uppermost mantle. 752
 However, the width of the UPMB has a strong influence on the
 753 localization of deformation for all thermal conditions of the
 754 uppermost mantle. Such model behaviour implies that even if
 755 the extensional velocity applied at the boundary of the model is
 756 constant, various strain rates in a significantly deformed region
 757 can be obtained, depending on the characteristics of the
 758 rheological heterogeneity brought about by the UPMB. 759
- (iii) For the model with a very wide UPMB, the effective strain rate
 760 is predicted to be very slow, and outward migration of
 761 deformation can be obtained in relation to thermal diffusion
 762 during the extensional process. However, such a migration is
 763 still limited to the region where the UPMB is situated. The
 764 outward migration of the deformation is also dependent on the
 765 thickness of the UPMB; a greater thickness of the UPMB is
 766 preferred for the outward migration. 767
- (iv) An UPMB in the lower crust could be an origin of a weak zone
 768 only when its temperature is significantly high. Once the UPMB
 769 loses the thermal anomaly, deformation would migrate to
 770 outside the UPMB. This is because a mafic lower crustal
 771 composition generally has more strength than a normal lower
 772 crustal composition without any thermal effects. 773

- (v) The relative importance of the UPMB to a locally thickened crust depends on the lateral scale of heterogeneity; if the upward migration of melts is concentrated into a region narrower than the lateral scale of the crustal heterogeneity, localization of the extensional deformation is dominantly controlled by the UPMB. When the variation in thickness of crust is small, the UPMB still plays a dominant role in localization of deformation, which is independent of the lateral scale of the UPMB.
- (vi) Lateral variation in the thickness of the UPMB can lead to asymmetric rift and passive margin structures. A greater amount of deformation is concentrated into the region where a larger amount of migrated magma has accumulated below the Moho. However, the greatest thickness of the UPMB must be away from the centre of the UPMB so as to obtain the asymmetric structure found in narrow volcanic and wide non-volcanic passive margins. It is also noted that an asymmetric rift structure is more favourably obtained by the UPMB when the strength contrast between each domain of the UPMB is weak enough not to distribute deformation into a particular domain. Although our numerical model shows the potential of UPMBs to produce an asymmetric rift structure, additional weakening may be required to obtain the lithosphere-cutting shear zone that is favourable for simple shear deformation.
- (vii) An UPMB that is emplaced during an extensional process results in deformation migration into a narrower region. This can be responsible for inward migration of deformation which could develop into a continental break-up as observed in continental rifts and passive margins. A small amount of UPMB emplaced in the uppermost mantle favours a localized break-up, whereas a huge amount may blur out the localization. The least amount of UPMB could result in successive localizations of deformation and magmatic activity into a more local region.

Acknowledgements

We would like to thank Peter Readman for carefully reading the manuscript and valuable suggestions. Giacomo Corti and an anonymous reviewer are acknowledged for constructive reviews of the manuscript. The calculations in this study were carried out on the computer facilities at the Dublin Institute for Advanced Studies and University College Dublin. TY thanks Kelin Wang for sharing the finite element code *tekton* ver.2.1 and for allowing modification of the code. Jay Melosh and Arthur Raefsky are also acknowledged as the authors of the original code. TY was supported by the CosmoGrid Project that is funded by the Program for Research in Third Level Institutions under the Irish National Development Plan and with assistance from the European Regional Development Fund.

References

- Artemjev, M.E., Artyushkov, E.V., 1971. Structure and isostasy of the Baikal Rift and the mechanism of rifting. *J. Geophys. Res.* 76, 1197–1211.
- Bassi, G., 1991. Factors controlling the style of continental rifting: insights from numerical modelling. *Earth Planet. Sci. Lett.* 105, 430–452.
- Bassi, G., 1995. Relative importance of strain rate and rheology for the mode of continental extension. *Geophys. J. Int.* 122, 195–210.
- Bassi, G., Keen, C.E., Potter, P., 1993. Contrasting styles of rifting: models and examples from the Eastern Canadian margin. *Tectonics* 12, 639–655.
- Bauer, K., Neben, S., Schreckenberger, B., Emmermann, R., Hinz, K., Fechner, N., Gohl, K., Schulze, A., Trumbull, R.B., Weber, K., 2000. Deep structure of the Namibian continental margin as derived from integrated geophysical studies. *J. Geophys. Res.* 105, 25,829–25,853.
- Berndt, C., Mjelde, R., Planke, S., Shimamura, H., Faleide, J.I., 2001. Controls on the tectono-magmatic evolution of a volcanic transform margin: the Vøring Transform Margin, NE-Atlantic. *Mar. Geophys. Res.* 22, 133–152.
- Bonini, M., Sokoutis, D., Mulugeta, G., Boccaletti, M., Corti, G., Innocenti, F., Manetti, P., Mazzarini, F., 2001. Dynamics of magma emplacement in the centrifuge models of continental extension with implications for flank volcanism. *Tectonics* 20, 1053–1065.

- Brace, W.F., Kohlstedt, D.L., 1980. Limits on lithospheric stress imposed by laboratory experiments. *J. Geophys. Res.* 85, 6248–6252. 840
- Braun, J., Beaumont, C., 1987. Styles of continental rifting: results from dynamic models of lithospheric extension. In: Beaumont, C., Tankard, A.J. (Eds.), *Sedimentary Basins and Basin-Forming Mechanisms*. Can. Soc. Pet. Geol. Mem., 12, pp. 241–258. 842
- Braun, J., Beaumont, C., 1989. Dynamic models of the role of crustal shear zones in asymmetric continental extension. *Earth Planet. Sci. Lett.* 93, 405–423. 844
- Buck, W.R., 1991. Modes of continental lithospheric extension. *J. Geophys. Res.* 96, 20,161–20,178. 845
- Buck, W.R., 2006. The role of magma in the development of the Afro-Arabian Rift System. In: Yirgu, G., Ebinger, C.J., Maguire, P.K.H. (Eds.), *The Afar Volcanic Province Within the East African Rift System*. Spec. Pub., 259. Geological Society of London, pp. 43–54. 848
- Burke, K., Dewey, J.F., 1973. Plume-generated triple junctions: key indicators in applying plate tectonics to old rocks. *J. Geol.* 81, 406–433. 849
- Burov, E., Guillou-Frottier, L., 2005. The plume head–continental lithosphere interaction using a tectonically realistic formulation for the lithosphere. *Geophys. J. Int.* 161, 469–490. 850
- Burov, E., Guillou-Frottier, L., d’Acremont, E., Le Pourhiet, L., Cloetingh, S., 2007. Plume head–lithosphere interactions near intra-continental plate boundaries. *Tectonophysics* 434, 15–38. 851
- Byerlee, J.D., 1967. Frictional characteristics of granite under high confining pressure. *J. Geophys. Res.* 72, 3639–3648. 852
- Byerlee, J.D., 1978. Friction of rocks. *Pure Appl. Geophys.* 116, 615–626. 853
- Callot, J.-P., Grigné, C., Geoffroy, L., Brun, J.-P., 2001. Development of volcanic passive margins: two-dimensional laboratory models. *Tectonics* 20, 148–159. 854
- Callot, J.-P., Geoffroy, L., Brun, J.-P., 2002. Development of volcanic passive margins: three-dimensional laboratory models. *Tectonics* 21 (1052). doi:10.1029/2001TC901019. 855
- Carter, N.L., Tsenn, M.C., 1987. Flow properties of continental lithosphere. *Tectonophysics* 136, 27–63. 856
- Chapman, D.S., Furlong, K.P., 1992. Thermal state of the lower continental crust. In: Fountain, D.M., Arculus, R., Kay, R.W. (Eds.), *Continental Lower Crust*. Elsevier, pp. 179–199. 857
- Chopra, P.N., Paterson, M.S., 1984. The role of water in the deformation of dunite. *J. Geophys. Res.* 89, 7861–7876. 858
- Coffin, M.F., Eldholm, O., 1994. Large igneous provinces: crustal structure, dimensions, and external consequences. *Rev. Geophys.* 32, 1–36. 859
- Corti, G., Manetti, P., 2006. Asymmetric rifts due to asymmetric Mohos: an experimental approach. *Earth Planet. Sci. Lett.* 245, 315–329. 860
- Corti, G., Bonini, M., Conticelli, S., Innocenti, F., Manetti, P., Sokoutis, D., 2003a. Analogue modelling of continental extension: a review focused on the relations between patterns of deformation and the presence of magma. *Earth Sci. Rev.* 63, 169–247. 861
- Corti, G., van Wijk, J., Bonini, M., Sokoutis, D., Cloetingh, S., Innocenti, F., Manetti, P., 2003b. Transition from continental break-up to punctiform seafloor spreading: how fast, symmetric and magmatic. *Geophys. Res. Lett.* 30 (1604). doi:10.1029/2003GL017374. 862
- Corti, G., Bonini, M., Innocenti, F., Manetti, P., Piccardo, G.B., Ranalli, G., 2007. Experimental models of extension of continental lithosphere weakened by percolation of asthenospheric melts. *J. Geodyn.* 43, 465–483. 863
- Courtillot, V.E., Renne, P.R., 2003. On the ages of flood basalt events. In: Courtillot, V.E. (Ed.), *The Earth’s Dynamics*. Comptes Rendus-Académic des Sciences. Geoscience, 335, pp. 113–140. 864
- Cox, K.G., 1980. A model for flood basalt volcanism. *J. Petrol.* 21, 629–650. 865
- Davis, M., Kusznir, N., 2004. Depth-dependent lithospheric stretching at rifted continental margins. In: Karner, G.D. (Ed.), *Proceedings of NSF Rifted Margins*. Theoretical Institute. Columbia University Press, pp. 92–136. 866
- Dunbar, J.A., Sawyer, D.S., 1988. Continental rifting at pre-existing lithospheric weaknesses. *Nature* 333, 450–452. 867
- Dunbar, J.A., Sawyer, D.S., 1989a. How preexisting weaknesses control the style of continental breakup. *J. Geophys. Res.* 94, 7278–7292. 868
- Dunbar, J.A., Sawyer, D.S., 1989b. Patterns of continental extension along the conjugate margins of the central and north Atlantic oceans and Labrador Sea. *Tectonics* 8, 1059–1077. 869
- Dobre, C., Manighetti, I., Dorbath, C., Dorbath, L., Jacques, E., Delmond, J.C., 2007a. Crustal structure and magmato-tectonic processes in an active rift (Asal-Ghoubbet, Afar, East Africa): 1. Insights from a 5-month seismological experiment. *J. Geophys. Res.* 112 (B05405). doi:10.1029/2005JB003940. 870
- Dobre, C., Manighetti, I., Dorbath, L., Dorbath, C., Bertil, D., Delmond, J.C., 2007b. Crustal structure and magmato-tectonic processes in an active rift (Asal-Ghoubbet, Afar, East Africa): 2. Insights from the 23-year recording of seismicity since the last rifting event. *J. Geophys. Res.* 112 (B05406). doi:10.1029/2006JB004333. 871
- Ebbing, J., Lundin, E., Olesen, O., Hansen, E.K., 2006. The mid-Norwegian margin: a discussion of crustal lineaments, mafic intrusions and remnants of the Caledonian root by 3D density modelling and structural interpretation. *J. Geol. Soc. (Lond.)* 163, 47–59. 872
- Ebinger, C.J., Casey, M., 2001. Continental breakup in magmatic provinces: an Ethiopian example. *Geology* 29, 527–530. 873
- Eldholm, O., Gladczenko, T.P., Skogseid, J., Planke, S., 2000. Atlantic volcanic margins: a comparative study. In: Nøttvedt, A. (Ed.), *Dynamics of the Norwegian Margin*. Spec. Pub. Geological Society of London, pp. 411–428. 874
- England, P., 1983. Constraints on extension of continental lithosphere. *J. Geophys. Res.* 88, 1145–1152. 875
- Fernández, M., Ranalli, G., 1997. The role of rheology in extensional basin formation modelling. *Tectonophysics* 282, 129–145. 876
- Fletcher, R.C., Hallet, B., 1983. Unstable extension of the lithosphere: a mechanical model for basin and range structure. *J. Geophys. Res.* 88, 7457–7466. 877

- Frederiksen, S., Braun, J., 2001. Numerical modelling of strain localization during extension of the continental lithosphere. *Earth Planet. Sci. Lett.* 188, 241–251.
- Frey, Ø., Planke, S., Symonds, P.A., Heeremans, M., 1998. Deep crustal structure and rheology of the Gascoyne volcanic margin, western Australia. *Mar. Geophys. Res.* 20, 293–312.
- Gac, S., Geoffroy, L., submitted for publication. Thermo-mechanical modelling in 3D of a stretched continental lithosphere containing localized low viscosity anomalies (the soft-point theory of plate break-up).
- Gans, P.B., 1987. An open-system, two-layer crustal stretching model for the eastern Great Basin. *Tectonics* 6, 1–12.
- Geoffroy, L., 2005. Volcanic passive margin. *C. R. Geosciences* 337, 1395–1408.
- Geoffroy, L., Callot, J.-P., Scaillet, S., Skuce, A.S., Gélard, J.P., Ravilly, M., Angelier, J., Bonin, B., Cayet, C., Perrot, K., Lepvrier, C., 2001. Southeast Baffin volcanic margin and the North American–Greenland plate separation. *Tectonics* 20, 566–584.
- Gernigon, L., Ringenbach, J.-C., Planke, S., Le Gall, B., 2004. Deep structures and breakup along volcanic rifted margins: insights from integrated studies along the outer Vøring Basin (Norway). *Mar. Pet. Geol.* 21, 363–372.
- Gernigon, L., Lucazeau, F., Brigaud, F., Ringenbach, J.-C., Planke, S., Le Gall, B., 2006. A moderate melting model for the Vøring margin (Norway) based on structural observations and a thermo-kinematic modelling: Implication for the meaning of the lower crustal bodies. *Tectonophysics* 412, 255–278.
- Gładczenko, T.P., Hinz, K., Eldholm, O., Meyer, H., Neben, S., Skogseid, J., 1997. South Atlantic volcanic margin. *J. Geol. Soc. (Lond.)* 154, 465–470.
- Govers, R., Wortel, M.J.R., 1993. Initiation of asymmetric extension in continental lithosphere. *Tectonophysics* 223, 75–96.
- Govers, R., Wortel, M.J.R., 1995. Extension of stable continental lithosphere and the initiation of lithospheric scale faults. *Tectonics* 14, 1041–1055.
- Govers, R., Wortel, M.J.R., 1999. Some remarks on the relation between vertical motions of the lithosphere during extension and the necking depth parameter inferred from kinematic modeling studies. *J. Geophys. Res.* 104, 23,245–23,253.
- Griffiths, R., Campbell, I., 1991. Interaction of mantle plume heads with the Earth's surface and onset of small-scale convection. *J. Geophys. Res.* 96, 18,295–18,310.
- Harry, D.L., Leeman, W.P., 1995. Partial melting of melt metasomatized subcontinental mantle and the magma source potential of the lower lithosphere. *J. Geophys. Res.* 100, 10,255–10,269.
- Harry, D.L., Sawyer, D.S., Leeman, W.P., 1993. The mechanics of continental extension in western North America: implications for the magmatic and structural evolution of the Great Basin. *Earth Planet. Sci. Lett.* 117, 59–71.
- Hayward, N., Ebinger, C., 1996. Variations in the along-axis segmentation of the Afar rift system. *Tectonics* 15, 244–257.
- Hirth, G., Kohlstedt, D.L., 1996. Water in the oceanic upper mantle: implications for rheology, melt extraction and the evolution of the lithosphere. *Earth Planet. Sci. Lett.* 144, 93–108.
- Huisman, R.S., Beaumont, C., 2002. Asymmetric lithospheric extension: the role of frictional-plastic strain softening inferred from numerical experiments. *Geology* 30, 211–214.
- Hutchinson, D.R., White, R.S., Cannon, W.F., Schulz, K.J., 1990. Keweenaw hot spot: geophysical evidence for a 1.1 Ga mantle plume beneath the Midcontinent Rift system. *J. Geophys. Res.* 95, 10,869–10,884.
- Keranen, K., Klemperer, S.L., Gloaguen, R., EAGLE Working Group, 2004. Three-dimensional seismic imaging of a protoridge axis in the Main Ethiopian rift. *Geology* 32, 949–952.
- Keir, D., Ebinger, C.J., Stuart, G.W., Daly, E., Ayele, A., 2006. Strain accommodation by magmatism and faulting as rifting proceeds to breakup: seismicity of the northern Ethiopian rift. *J. Geophys. Res.* 111 (B05314). doi:10.1029/2005JB003748.
- Kirby, S.H., 1983. Rheology of the lithosphere. *Rev. Geophys. Space Phys.* 21, 1458–1487.
- Klausen, M.B., Larsen, H.C., 2002. East Greenland coast-parallel dike swarm and its role in continental breakup. In: Menzies, M.A., Klemperer, S.L., Ebinger, C.J., Baker, J. (Eds.), *Volcanic Rifted Margins: Boulder, Colorado*. Spec. Pub., vol. 362. Geol. Soc. Am., pp. 137–200.
- Koch, P.S., Christie, J.M., Ord, A., George Jr., R.P., 1989. Effect of water on the rheology of experimentally deformed quartzite. *J. Geophys. Res.* 94, 13,975–13,996.
- Kusznir, J.N., Egan, S.S., 1989. Simple shear and pure shear models of extensional sedimentary basin formation: application to the Jeanne d'Arc basin, grand banks of Newfoundland. *Mem. – Am. Assoc. Pet. Geol.* 46, 305–322.
- Lachenbruch, A.H., Sass, J.H., 1978. Models of an extending lithosphere and heat flow in the Basin and Range Province. In: Smith, R., Eaton, G. (Eds.), *Cenozoic Tectonics and Regional Geophysics of the Western Cordillera*. Mem. Geol. Soc. Am., vol. 152, pp. 209–250.
- Lachenbruch, A.H., Morgan, P., 1990. Continental extension, magmatism and elevation: formal relations and rules of thumb. *Tectonophysics* 174, 39–62.
- Laske, G., Masters, G., 1997. A global digital map of sediment thickness. *EOS Trans. AGU* 78 (F483).
- Latin, D., White, N., 1990. Generating melt during lithospheric extension: pure shear vs. simple shear. *Geology* 18, 327–331.
- Lister, G.S., Davis, G.A., 1989. The origin of metamorphic core complexes and detachment faults formed during Tertiary continental extension in the northern Colorado River region U.S.A. *J. Struct. Geol.* 11, 65–94.
- Lister, G.S., Etheridge, M.A., Symonds, P.A., 1991. Detachment models for the formation of passive continental margins. *Tectonics* 10, 1038–1064.
- Lizarralde, D., Axen, G.J., Brown, H.E., Fletcher, J.M., González-Fernández, A., Harding, A.J., Holbrook, W.S., Kent, G.M., Paramo, P., Sutherland, F., Umhoefer, P.J., 2007. Variation in styles of rifting in the Gulf of California. *Nature* 448. doi:10.1038/nature06035.
- Maguire, P.K.H., Keller, G.R., Klemperer, S.L., Mackenzie, G.D., Keranen, K., Harder, S., O'Reilly, B., Thybo, H., Asfaw, L., Khan, M.A., Amha, M., 2006. Crustal structure of the Northern Main Ethiopian Rift from the EAGLE controlled source survey: a snapshot of incipient lithospheric break-up. In: Yirgu, G., Ebinger, C., Maguire, P.K.H. (Eds.), *The Afar volcanic province within the East African Rift System*. Spec. Pub., vol. 259. Geol. Soc. Lond., pp. 269–291.
- Manighetti, I., Tapponnier, P., Courtillot, V., Gruszow, S., Gillot, P.-Y., 1998. Propagation of rifting along the Arabia–Somalia plate boundary. *J. Geophys. Res.* 102, 2681–2710.
- McKenzie, D.P., 1978. Some remarks on the development of sedimentary basins. *Earth Planet. Sci. Lett.* 40, 25–32.
- McKenzie, D., Bickle, J.M., 1988. The volume and composition of melt generated by extension of the lithosphere. *J. Petrol.* 29, 625–679.
- Mackenzie, G.D., Thybo, H., Maguire, P.K.H., 2005. Crustal velocity structure across the Main Ethiopian Rift: results from two-dimensional wide-angle seismic modelling. *Geophys. J. Int.* 162, 994–1006.
- Melosh, H.J., Raefsky, A., 1980. The dynamical origin of subduction zone topography. *Geophys. J. R. Astron. Soc.* 60, 333–354.
- Melosh, H.J., Raefsky, A., 1981. A simple and efficient method for introducing faults into finite element computations. *Bull. Seismol. Soc. Am.* 71, 1391–1400.
- Melosh, H.J., Williams, C.A., 1989. Mechanics of graben formation in crustal rocks: a finite element analysis. *J. Geophys. Res.* 94, 13,961–13,973.
- Menzies, M.A., Klemperer, S.L., Ebinger, C.J., Baker, J., 2002. Characteristic of volcanic rifted margins. In: Menzies, M.A., Klemperer, S.L., Ebinger, C.J., Baker, J. (Eds.), *Volcanic Rifted Margins: Boulder, Colorado*. Spec. Pub., 362. Geol. Soc. Am., pp. 1–14.
- Mjelde, R., Raum, T., Murai, Y., Takanami, T., 2007. Continent-ocean-transitions: review, and a new tectono-magmatic model of the Vøring Plateau, NE Atlantic. *J. Geodyn.* 43, 374–392.
- Mohr, P., 1992. Nature of the crust beneath magmatically active continental rifts. *Tectonophysics* 213, 269–284.
- Müller, R.D., Roest, W.R., Royer, J.Y., Gahagan, L.M., Sclater, J.G., 1997. Digital isochrons of the world's ocean floor. *J. Geophys. Res.* 102, 3211–3214.
- Müller, R.D., Gaina, C., Roest, W.R., Hansen, D.L., 2001. A recipe for microcontinent formation. *Geology* 29, 203–206.
- Mutter, C.Z., Talwani, M., Stoffa, P., 1984. Evidence for thick oceanic crust adjacent to the Norwegian margin. *J. Geophys. Res.* 89, 483–502.
- Negredo, A.M., Fernández, M., Zeyen, H., 1995. Thermo-mechanical constraints on kinematic models of lithospheric extension. *Earth Planet. Sci. Lett.* 134, 87–98.
- Neumann, E.-R., Olsen, K.H., Baldrige, W.S., 1995. The Oslo rift. In: Olsen, K.H. (Ed.), *Continental Rifts: Evolution, Structure, Tectonics*. Developments in Geotectonics, vol. 25. Elsevier, pp. 345–371.
- Pascal, C., van Wijk, J.C., Cloetingh, S.A.P.L., Davies, G.R., 2002. Effect of lithosphere thickness heterogeneities in controlling rift localization: numerical modeling of the Oslo Graben. *Geophys. Res. Lett.* 29. doi:10.1029/2001GL014354.
- Planke, S., Skogseid, J., Eldholm, O., 1991. Crustal structure off Norway, 62° to 70° north. *Tectonophysics* 189, 91–107.
- Poliakov, A., Buck, R., 1998. Mechanics of stretching elastic-plastic-viscous layers: applications to slow-spreading mid-ocean ridges. In: Buck, R. (Ed.), *Faulting and Magmatism at Mid-Ocean Ridges*. Geophys. Mon., vol. 106. American Geophysical Union, pp. 305–324.
- Ranalli, G., 1995. *Rheology of the Earth*, 2nd ed. Chapman and Hall, London, p. 413.
- Ranalli, G., Piccardo, G.B., Corona-Chávez, P., 2007. Softening of the subcontinental lithospheric mantle by asthenosphere melts and the continental extension/oceanic spreading transition. *J. Geodyn.* 43, 450–464.
- Rey, P., 1993. Seismic and tectono-metamorphic characters of the lower continental crust in Phanerozoic areas: a consequence of postthickening extension. *Tectonics* 12, 580–590.
- Ro, H.E., Faleide, J.I., 1992. A stretching model for the Oslo Rift. *Tectonophysics* 208, 19–36.
- Royden, L., Keen, C.E., 1980. Rifting process and thermal evolution of the continental margin of eastern Canada determined from subsidence curves. *Earth Planet. Sci. Lett.* 51, 343–361.
- Ruppel, C., 1995. Extensional processes in continental lithosphere. *J. Geophys. Res.* 100, 24,187–24,215.
- Sengör, A.M.C., Burke, K., 1978. Relative timing of rifting and volcanism on earth and its tectonic implications. *Geophys. Res. Lett.* 5, 419–421.
- Shelton, G., Tullis, J., 1981. Experimental flow laws for crustal rocks. *EOS* 62, 396.
- Sigmundsson, F., 2006. Magma does the splits. *Nature* 442, 251–252.
- Speight, J., Skelhorn, R., Sloan, T., Knapp, R., 1982. The dyke swarms of Scotland. In: Sutherland, D.S. (Ed.), *Igneous Rocks of the British Isles*. John Wiley, London, pp. 449–459.
- Symonds, P.A., Planke, S., Frey, F., Skogseid, J., 1998. Volcanic evolution of the Western Australian continental margin and its implications for basin development. In: Purcell, P.G., Purcell, R.R. (Eds.), *The Sedimentary Basins of Western Australia 2: Proceedings of Petroleum Exploration Society of Australia Symposium*. Perth, pp. 33–34.
- Thompson, G.A., McCarthy, J., 1990. A gravity constraint on the origin of highly extended terranes. *Tectonophysics* 174, 197–206.
- Tirel, C., Brun, J.-P., Sokoutis, D., 2006. Extension of thickened and hot lithospheres: inferences from laboratory modeling. *Tectonics* 25 (TC1005). doi:10.1029/2005TC001804.
- Tucholke, B.E., Sawyer, D.S., Sibuet, J.-C., 2007. Breakup of the Newfoundland–Iberia rift. In: Karner, G.D., Manatschal, G., Pinheiro, L.M. (Eds.), *Imaging, Mapping and Modelling Continental Lithosphere Extension and Breakup*. Spec. Pub., vol. 282. Geol. Soc. Lond., pp. 9–46.
- van Wijk, J.W., Cloetingh, S.A.P.L., 2002. Basin migration caused by slow lithospheric extension. *Earth Planet. Sci. Lett.* 198, 275–288.
- Wernicke, B., 1985. Uniform-sense normal simple shear of the continental lithosphere. *Can. J. Earth Sci.* 22, 108–125.
- White, R., McKenzie, D., 1989. Magmatism at rift zones: the generation of volcanic continental margins and flood basalts. *J. Geophys. Res.* 94, 7685–7729.

- 1098 Williams, C.A., Richardson, R.M., 1991. A rheologically layered three-dimensional model 1106
1099 of the San Andreas fault in central and southern California. *J. Geophys. Res.* 96, 1107
1100 16,597–16,623.
- 1101 Wright, T.J., Ebinger, C., Biggs, J., Ayele, A., Yirgu, G., Keir, D., Stork, A., 2006. Magma- 1108
1102 maintained rift segmentation at continental rupture in the 2005 Afar dyking 1109
1103 episode. *Nature* 442, 291–294.
- 1104 Yamada, Y., Nakada, M., 2006. Stratigraphic architecture of sedimentary basin induced 1111 Q2
1105 by mantle diapiric upwelling and eustatic event. *Tectonophysics* 415, 103–121. 1112
1113
- Yamasaki, T., 2004. Localized rheological weakening by grain-size reduction during 1106
lithospheric extension. *Tectonophysics* 386, 117–145. 1107
- Yamasaki, T., O'Reilly, B., Readman, P., 2006. A rheological weak zone intensified by post- 1108
rift thermal relaxation as a possible origin of simple shear deformation associated 1109
with reactivation of rifting. *Earth Planet. Sci. Lett.* 248, 134–146. 1110
- Yamasaki, T., Miura, H., Nogi, Y., submitted for publication. Numerical modelling study 1111 Q2
on the flexural uplift of the Transantarctic Mountains. 1112
1113

1114

UNCORRECTED PROOF